Physics – Uspekhi **65** (7) 653 – 676 (2022)

REVIEWS OF TOPICAL PROBLEMS PACS numbers: **12.15. – y**, **12.60. – i**, 14.80.Bn

The SMEFT formalism: the basis for finding deviations from the Standard Model

E E Boos

DOI: https://doi.org/10.3367/UFNe.2021.02.038916

Contents

Abstract. The search for manifestations of physics beyond the Standard Model (SM) is one of the main directions of research at the LHC and future colliders under discussion. The effects caused by the new physics can consist in the direct detection of new particles if their masses are less than the characteristic energies available at colliders and their interactions with the SM particles are strong enough. But if the masses of new particles are too large, or the interactions with SM particles are too weak, then new particles cannot be detected directly. In this case, the new physics can lead to a modification of the interactions of SM particles, to subthreshold effects. We present the current status of an approach or formalism called the Standard Model Effective Field Theory (SMEFT), which allows us to describe and model deviations from the SM predictions in a theoretically consistent manner. The advantages of and serious problems with this approach are discussed.

Keywords: Standard Model, effective field theory, top quark, Higgs boson, higher-dimensional operators, unitarity, renormalizability

E E Boos
Lomonosov Moscow State University,
Skobeltsyn Institute of Nuclear Physics,
Leninskie gory 1, str. 2, 119991 Moscow, Russian Federation.
E-mail: boos@theory.sinp.msu.ru, Eduard.Boos@cern.ch

Received 21 December 2020, revised 18 January 2021
Uspekhi Fizicheskikh Nauk **192** (7) 697 – 721 (2022)
Translated by S Alekseev

1. Introduction

Currently, the theoretical description of the processes of interaction of elementary particles is provided by the Standard Model (SM), which is a gauge theory of strong, electromagnetic, and weak interactions with the electroweak symmetry group spontaneously broken via the Higgs mechanism. The SM is well confirmed experimentally: all the particles included in it have been discovered and studied, and theoretical calculations in the SM framework describe almost all experimental data very well. However, there are serious experimental and theoretical grounds to believe that the SM cannot be the ultimate theory of elementary particle interactions, and it must be modified or supplemented. In particular, the inaccuracy in experimental data leaves room for modifications of the scalar sector of the SM, which is currently chosen to be minimal, but is not rigorously fixed by any theoretical argument.

Attempts to generalize the SM have been ongoing for almost 50 years, including the construction of grand unification models and supersymmetric extensions of the SM, and models with extra space–time dimensions and with the presence of new superstrong interactions. However, there is still no realistic theory of interactions of elementary particles beyond the SM whose implications would be confirmed experimentally. Extensive efforts of experimentalists and theorists are concentrated on the search for phenomena beyond the SM framework and on the construction of the corresponding extensions of the SM.

Before the discovery of the Higgs boson at the Large Hadron Collider (LHC), important arguments regarding the possible scale of new physics (NP) were associated with the

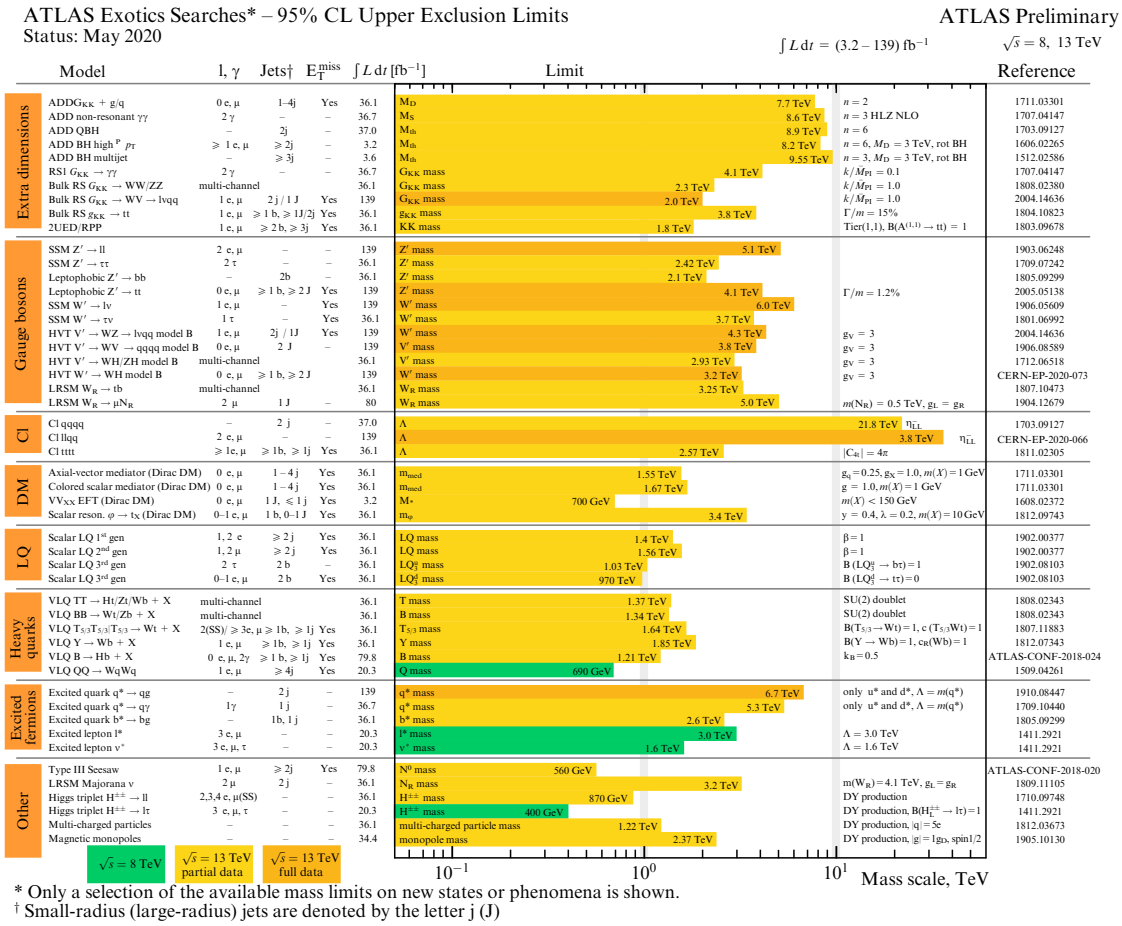

Figure 1. (Color online.) Bounds on parameters arising in SM extensions obtained by the ATLAS collaboration in the second run of the LHC at an energy of 13 TeV [8].

so-called No-Lose Theorem [1–4]. Based on an analysis of the behavior of the amplitudes of processes involving the longitudinal components of the massive gauge bosons in the SM, this theorem stated that two options are possible: either there must be a fairly light Higgs boson, with a mass up to about 700 GeV, or some new physics must appear on an energy scale of the order of 1 TeV, which would then lead to the restoration of the unitary behavior of the amplitudes. In 2012, the Higgs boson was discovered [5, 6], which was a triumph for the SM, confirming the mechanism of spontaneous gauge symmetry breaking. But the argument about a new scale of physics beyond the SM was then lost.

Another argument in favor of a scale of the order of 1 TeV before the discovery of the Higgs boson at the LHC was that the total decay width of the Higgs boson with a mass M_H greater than the mass of two W bosons increases proportionally to M_H^3 and at boson masses of the order of 1 TeV becomes comparable to the mass itself. This also indicated that, if the Higgs boson with a significantly lower mass had not been found, then the SM would have become inapplicable on a scale of the order of 1 TeV and some kind of NP should appear. But the Higgs boson with a mass of about 125 GeV was found, and this argument about a new scale was also dropped.

The well-known hierarchy problem associated with corrections to the squared mass of the Higgs boson does not provide new arguments for the existence of a distinguished scale either: the coupling constant of a hypothetical new particle with the Higgs boson can be very small, and the corresponding loop corrections to the squared mass of the Higgs boson can also be very small, even for a very heavy new particle.

Of course, we know that Planck's gravitational scale is about 10^{19} GeV. It is also known that, on the so-called grand unification scale of the order of 10^{16} GeV, the curves showing the behavior of the running gauge coupling constants intersect, albeit not quite exactly. Small neutrino masses may be associated with a scale of the order of 10^{11}–10^{12} GeV. But we presently do not know whether a new scale of the order of tens or several tens of TeV exists, available for studies at the LHC or at the Future Circular Collider (FCC). Even today, the mass bounds for a number of new particles predicted in models beyond the SM exceed one or several TeV [7], as is demonstrated in Fig. 1 [8] and Fig. 2 [9] obtained by the ATLAS (A Toroidal LHC ApparatuS) and CMS (Compact Muon Solenoid) collaborations in the second run of the LHC at an energy of 13 TeV.

Depending on the relations among the energies available at accelerators/colliders and the characteristic scale of NP, there are two main strategies to search for its manifestations: a direct search for new particles if their masses are such that the collider energies are sufficient for their creation and if these new objects are coupled strongly enough to SM particles for the luminosity of the collider to allow their detection, or the search for deviations from SM predictions in precision measurements if the masses of new particles are greater than

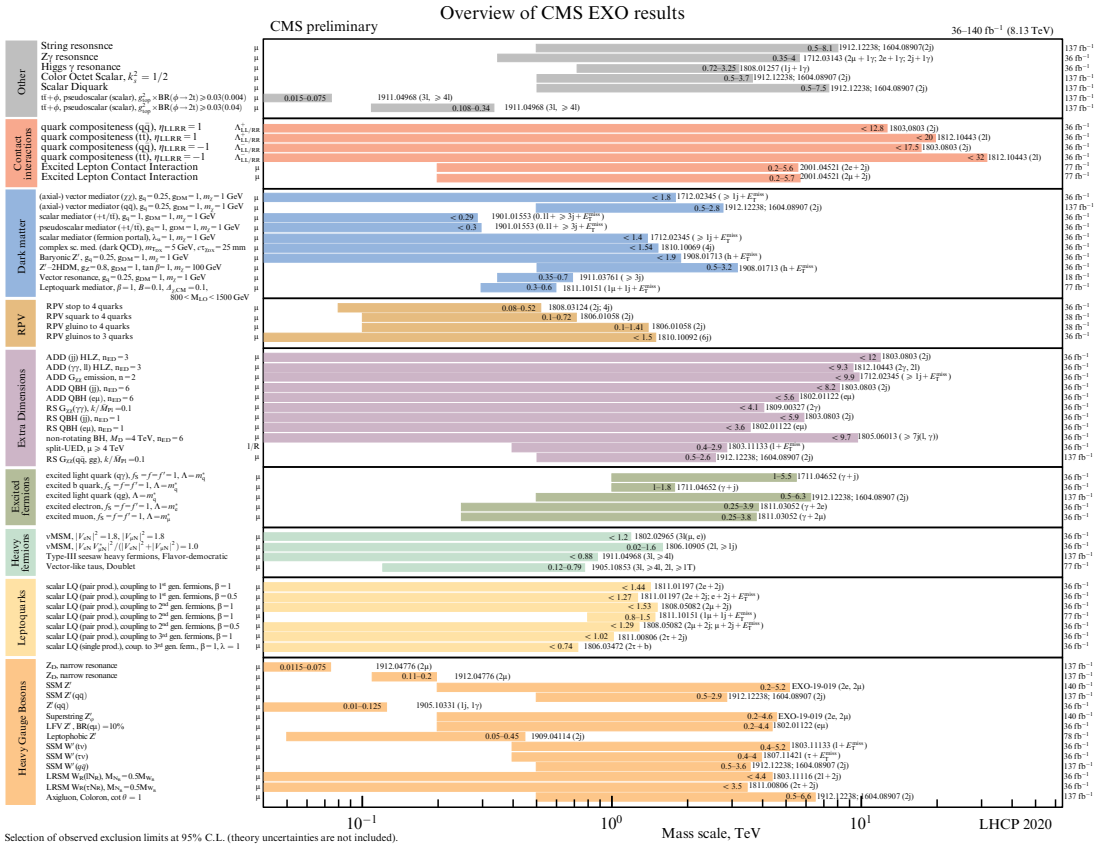

Figure 2. (Color online.) Bounds on parameters arising in SM extensions obtained by the CMS collaboration in the second run of the LHC at an energy of 13 TeV [9].

the characteristic attainable energies at colliders. In the latter case, the effects of new particles can manifest themselves in loop corrections to the SM processes or due to subthreshold contributions, which would lead to changes in the characteristics of the processes, including cross sections, differential distributions, widths, and decay branching ratios. These two possibilities are symbolically depicted in Fig. 3.

In the current situation, when no direct production of new particles has been discovered, studies of this second possibility are of particular importance, and hence indirect searches for deviations from the SM have recently attracted increased attention of the scientific community.

The main approach for studying indirect manifestations of new particles and new interactions is provided by effective field theories constructed on the basis of higher-dimensional effective operators that preserve the SM symmetries. This brief review is devoted to the description of a model-independent formalism for parameterizing deviations from the SM, called the Standard Model Effective Field Theory (SMEFT), and to the application of this formalism to the LHC data analysis.

We discuss the advantages of and serious problems with this approach. An undoubted advantage of the SMEFT formalism is that it is a consistent field-theory approach that preserves the gauge symmetry and other SM symmetries. SMEFT allows calculating perturbative corrections in the SM coupling constants. In each order in the inverse-squared scale, there are numerous, but a finite number of, independent gauge-invariant operators. Therefore, in calculating loop corrections, all counterterms are expressed in terms of the

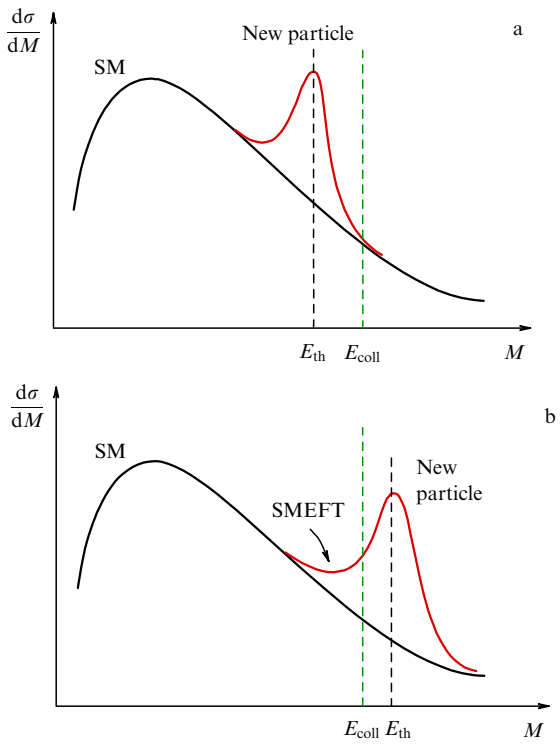

Figure 3. Two possible situations in the distribution over a conventional variable of dimension mass, when the characteristic collision energy is (a) greater or (b) less than the new-physics threshold.

same set of operators, which allows the renormalization procedure to be implemented, even though by formal power-counting the SMEFT Lagrangian belongs to the class of nonrenormalizable ones. At the same time, the number of independent operators, even in the minimal basis, is very large, which makes calculations and analysis difficult. Renormalizations lead to further complications by mixing operator contributions to the observables. Great care must be taken in specific applications in order not to let the calculations enter kinematical regions where the SMEFT approach is inapplicable due to unitarity violation. In cases where several operators contribute to the same observables, calculations can in principle lead to 'flat' directions in the parameter space, when constraints on the corresponding combinations of parameters simply do not arise. Such cases require a joint analysis of several processes, which is quite difficult to implement in real experiments.

This review is organized as follows. In Section 2, we discuss the main ideas of the SMEFT approach and briefly list the problems that arise when using it. Section 3 is devoted to the problem of choosing a minimal basis; we discuss a specific basis of operators, called the Warsaw basis, which, by convention, is largely adopted by the world community. In Section 4, we discuss the problem of taking $1/\Lambda^4$ contributions into account and the ensuing issues. The problem of perturbative corrections to the SMEFT tree contributions in higher orders in the SM coupling constants is discussed in Section 5. The application of the SMEFT formalism to studies of the Higgs boson and t-quark interactions is considered in Sections 6 and 7, respectively. Constraints on the Wilson coefficients that follow from the simultaneous analysis of different data or, as this is customarily called, from global data fitting, are given and discussed in Section 8. In Section 9, using some examples, we discuss effective operators of dimension 6 that follow from specific models when integrating out heavy degrees of freedom. It is shown that the emerging operators are a subset of the full set of SMEFT operators, and these operators themselves and the experimental bounds on the corresponding Wilson coefficients can testify in favor of one model or another beyond the SM if deviations from the SM are found. Concluding remarks are given in Section 10.

2. Main ideas of the SMEFT formalism

The basis of the formalism is an effective field theory (EFT) that describes deviations from the SM by an effective Lagrangian, in which these deviations are parameterized by gauge-invariant local operators with increasing dimensions exceeding 4. The operators themselves are composed of the SM fields; in the SMEFT Lagrangian, the sum of terms that are products of operators and some coefficients is added to the SM Lagrangian. These coefficients are proportional to dimensionless constants, called Wilson coefficients, and to some inverse power of the possible NP scale, so as to ensure that the total dimension of each term in the Lagrangian is equal to 4. Taking the contributions of operators to observables into account leads to corrections and hence to predictions of deviations from the SM. The search for predicted deviations against the background of SM contributions allows either detecting them or imposing bounds on the coefficients at the operators.

Recently, this approach, which goes back to the work of Weinberg [10] and Buchmüller–Wyler [11], was named the SMEFT. The SMEFT Lagrangian has the form

$$\mathcal{L}_{\mathrm{SMEFT}} = \mathcal{L}_{\mathrm{SM}} + \sum_i \frac{C_i^{(6)}}{\Lambda^2} O_i^{(6)} + \sum_j \frac{C_j^{(8)}}{\Lambda^4} O_j^{(8)} + \ldots, \quad (1)$$

where $O_i^{(6)}$, $O_j^{(8)}$, ... are gauge-invariant operators with increasing dimension, $C_i^{(6)}$, $C_j^{(8)}$, ... are the corresponding Wilson coefficients, and Λ is the characteristic NP scale.

The idea of SMEFT is based on the so-called decoupling theorem [12], which asserts that "for any 1PI Feynman graph with external vector mesons only but containing internal fermions, when all external momenta (p^2) are small relative to m^2, then apart from coupling constant and field strength renormalization the graph will be suppressed by some power of m relative to a graph with the same number of external vector mesons but no internal fermions."

This theorem actually follows from the proof of the local structure of counterterms proposed by Bogoliubov and Parasiuk [13] in 1957. At present, the decoupling theorem is better known as integrating out heavy particles.

The formulation of the SMEFT in the form of effective Lagrangian (1) looks very simple, but in practice entails a number of serious problems. The main problems are listed below.

- The problem of choosing a basis of independent operators.
- When calculating the characteristics of processes, leading contributions of the order of $1/\Lambda^2$ arise from the interference of the contributions of operators of dimension 6 and SM contributions. This raises the question of whether the contributions of the squared dimension-six operators of the order of $1/\Lambda^4$ must be taken into account when they arise in calculating the squared amplitudes of physical processes.
- Is it justified to calculate perturbative corrections in the strong and electroweak SM coupling constants in a formally nonrenormalizable field theory, such as the SMEFT?
- How do we deal with the unitarity problem in the case where the contributions of higher-dimension operators can lead to nonunitary behavior of cross sections?
- What should the correct modeling of processes be, and what is the strategy for obtaining the bounds on the Wilson coefficients in analyzing experimental data?

We address these questions in detail in Sections 3–8.

3. Choosing a basis of operators

The operator basis consists of symmetry-allowed operators, whose number is reduced to a minimum by using equations of motion, integration by parts, and Fierz rearrangements.

As is well known, there is only one operator of dimension five, called the Weinberg operator [10], which consists of a left electroweak lepton doublet, the conjugate left doublet of leptons, a Higgs field doublet, and its charge-conjugate doublet. This operator is very interesting for neutrino physics, but its contribution is insignificant for collider physics.

One of the first classifications of dimension-six operators was proposed by Buchmüller and Wyler [11]. Subsequently, the number of independent operators was reduced. A new basis, called the Warsaw basis, was proposed in 2010 by Grzadkowski, Iskrzynski, Misiak, and Rosiek [14] and is presented in Table 1.

The notation used in Table 1 corresponds exactly to the original notation in [14]: H is the Higgs field doublet,

Table 1. Warsaw basis operators. Fifty-nine independent symmetry-preserving SM operators of dimension 6, divided into eight classes, are presented in the original notation [14]. Notation + h.c. means the addition of the Hermitian-conjugate part. Subscripts p, r, s, t correspond to the generation numbers.

$1 : X^3$	
O_G	$f^{ABC} G_\mu^{A\nu} G_\nu^{B\rho} G_\rho^{C\mu}$
$O_{\tilde{G}}$	$f^{ABC} \widetilde{G}_\mu^{A\nu} G_\nu^{B\rho} G_\rho^{C\mu}$
O_W	$\epsilon^{IJK} W_\mu^{I\nu} W_\nu^{J\rho} W_\rho^{K\mu}$
$O_{\tilde{W}}$	$\epsilon^{IJK} \widetilde{W}_\mu^{I\nu} W_\nu^{J\rho} W_\rho^{K\mu}$

$2 : H^6$	
O_H	$(H^\dagger H)^3$

$3 : H^4 D^2$	
$O_{H\Box}$	$(H^\dagger H)\Box(H^\dagger H)$
O_{HD}	$(H^\dagger D_\mu H)^*(H^\dagger D_\mu H)$

$5 : \psi^2 H^3 + \text{h.c.}$	
O_{eH}	$(H^\dagger H)(\bar{l}_p e_r H)$
O_{uH}	$(H^\dagger H)(\bar{q}_p u_r \tilde{H})$
O_{dH}	$(H^\dagger H)(\bar{q}_p d_r H)$

$4 : X^2 H^2$	
O_{HG}	$H^\dagger H G_{\mu\nu}^A G^{A\mu\nu}$
$O_{H\tilde{G}}$	$H^\dagger H \widetilde{G}_{\mu\nu}^A G^{A\mu\nu}$
O_{HW}	$H^\dagger H W_{\mu\nu}^I W^{I\mu\nu}$
$O_{H\tilde{W}}$	$H^\dagger H \widetilde{W}_{\mu\nu}^I W^{I\mu\nu}$
O_{HB}	$H^\dagger H B_{\mu\nu} B^{\mu\nu}$
$O_{H\tilde{B}}$	$H^\dagger H \widetilde{B}_{\mu\nu} B^{\mu\nu}$
O_{HWB}	$H^\dagger \tau^I H W_{\mu\nu}^I B^{\mu\nu}$
$O_{H\tilde{W}B}$	$H^\dagger \tau^I H \widetilde{W}_{\mu\nu}^I B^{\mu\nu}$

$6 : \psi^2 XH + \text{h.c.}$	
O_{eW}	$(\bar{l}_p \sigma^{\mu\nu} e_r) \tau^I H W_{\mu\nu}^I$
O_{eB}	$(\bar{l}_p \sigma^{\mu\nu} e_r) H B_{\mu\nu}$
O_{uG}	$(\bar{q}_p \sigma^{\mu\nu} T^A u_r) \tilde{H} G_{\mu\nu}^A$
O_{uW}	$(\bar{q}_p \sigma^{\mu\nu} u_r) \tau^I \tilde{H} W_{\mu\nu}^I$
O_{uB}	$(\bar{q}_p \sigma^{\mu\nu} u_r) \tilde{H} B_{\mu\nu}$
O_{dG}	$(\bar{q}_p \sigma^{\mu\nu} T^A d_r) H G_{\mu\nu}^A$
O_{dW}	$(\bar{q}_p \sigma^{\mu\nu} d_r) \tau^I H W_{\mu\nu}^I$
O_{dB}	$(\bar{q}_p \sigma^{\mu\nu} d_r) H B_{\mu\nu}$

$7 : \psi^2 H^2 D$	
$O_{Hl}^{(1)}$	$(H^\dagger \mathrm{i} \overleftrightarrow{D}_\mu H)(\bar{l}_p \gamma^\mu l_r)$
$O_{Hl}^{(3)}$	$(H^\dagger \mathrm{i} \overleftrightarrow{D}_\mu^I H)(\bar{l}_p \tau^I \gamma^\mu l_r)$
O_{He}	$(H^\dagger \mathrm{i} \overleftrightarrow{D}_\mu H)(\bar{e}_p \gamma^\mu e_r)$
$O_{Hq}^{(1)}$	$(H^\dagger \mathrm{i} \overleftrightarrow{D}_\mu H)(\bar{q}_p \gamma^\mu q_r)$
$O_{Hq}^{(3)}$	$(H^\dagger \mathrm{i} \overleftrightarrow{D}_\mu^I H)(\bar{q}_p \tau^I \gamma^\mu q_r)$
O_{Hu}	$(H^\dagger \mathrm{i} \overleftrightarrow{D}_\mu H)(\bar{u}_p \gamma^\mu u_r)$
O_{Hd}	$(H^\dagger \mathrm{i} \overleftrightarrow{D}_\mu H)(\bar{d}_p \gamma^\mu d_r)$
$O_{Hud} + \text{h.c.}$	$\mathrm{i}(\tilde{H}^\dagger D_\mu H)(\bar{u}_p \gamma^\mu d_r)$

$8 : (\bar{\mathrm{L}}\mathrm{L})(\bar{\mathrm{L}}\mathrm{L})$	
O_{ll}	$(\bar{l}_p \gamma_\mu l_r)(\bar{l}_s \gamma^\mu l_t)$
$O_{qq}^{(1)}$	$(\bar{q}_p \gamma_\mu q_r)(\bar{q}_s \gamma^\mu q_t)$
$O_{qq}^{(3)}$	$(\bar{q}_p \gamma_\mu \tau^I q_r)(\bar{q}_s \gamma^\mu \tau^I q_t)$
$O_{lq}^{(1)}$	$(\bar{l}_p \gamma_\mu l_r)(\bar{q}_s \gamma^\mu q_t)$
$O_{lq}^{(3)}$	$(\bar{l}_p \gamma_\mu \tau^I l_r)(\bar{q}_s \gamma^\mu \tau^I q_t)$

$8 : (\bar{\mathrm{R}}\mathrm{R})(\bar{\mathrm{R}}\mathrm{R})$	
O_{ee}	$(\bar{e}_p \gamma_\mu e_r)(\bar{e}_s \gamma^\mu e_t)$
O_{uu}	$(\bar{u}_p \gamma_\mu u_r)(\bar{u}_s \gamma^\mu u_t)$
O_{dd}	$(\bar{d}_p \gamma_\mu d_r)(\bar{d}_s \gamma^\mu d_t)$
O_{eu}	$(\bar{e}_p \gamma_\mu e_r)(\bar{u}_s \gamma^\mu u_t)$
O_{ed}	$(\bar{e}_p \gamma_\mu e_r)(\bar{d}_s \gamma^\mu d_t)$
$O_{ud}^{(1)}$	$(\bar{u}_p \gamma_\mu u_r)(\bar{d}_s \gamma^\mu d_t)$
$O_{ud}^{(8)}$	$(\bar{u}_p \gamma_\mu T^A u_r)(\bar{d}_s \gamma^\mu T^A d_t)$

$8 : (\bar{\mathrm{L}}\mathrm{L})(\bar{\mathrm{R}}\mathrm{R})$	
O_{le}	$(\bar{l}_p \gamma_\mu l_r)(\bar{e}_s \gamma^\mu e_t)$
O_{lu}	$(\bar{l}_p \gamma_\mu l_r)(\bar{u}_s \gamma^\mu u_t)$
O_{ld}	$(\bar{l}_p \gamma_\mu l_r)(\bar{d}_s \gamma^\mu d_t)$
O_{qe}	$(\bar{q}_p \gamma_\mu q_r)(\bar{e}_s \gamma^\mu e_t)$
$O_{qu}^{(1)}$	$(\bar{q}_p \gamma_\mu q_r)(\bar{u}_s \gamma^\mu u_t)$
$O_{qu}^{(8)}$	$(\bar{q}_p \gamma_\mu T^A q_r)(\bar{u}_s \gamma^\mu T^A u_t)$
$O_{qd}^{(1)}$	$(\bar{q}_p \gamma_\mu q_r)(\bar{d}_s \gamma^\mu d_t)$
$O_{qd}^{(8)}$	$(\bar{q}_p \gamma_\mu T^A q_r)(\bar{d}_s \gamma^\mu T^A d_t)$

$8 : (\bar{\mathrm{L}}\mathrm{R})(\bar{\mathrm{R}}\mathrm{L}) + \text{h.c.}$	
O_{ledq}	$(\bar{l}_p^j e_r)(\bar{d}_s q_{tj})$

$8 : (\bar{\mathrm{L}}\mathrm{R})(\bar{\mathrm{L}}\mathrm{R}) + \text{h.c.}$	
$O_{quqd}^{(1)}$	$(\bar{q}_p^j u_r) \epsilon_{jk} (\bar{q}_s^k d_t)$
$O_{quqd}^{(8)}$	$(\bar{q}_p^j T^A u_r) \epsilon_{jk} (\bar{q}_s^k T^A d_t)$
$O_{lequ}^{(1)}$	$(\bar{l}_p^j e_r) \epsilon_{jk} (\bar{q}_s^k u_t)$
$O_{lequ}^{(3)}$	$(\bar{l}_p^j \sigma_{\mu\nu} e_r) \epsilon_{jk} (\bar{q}_s^k \sigma^{\mu\nu} u_t)$

$\tilde{H} = \varepsilon H^*$ is the conjugate Higgs field doublet expressed in terms of the antisymmetric tensor of the SU(2) group, in turn expressed in terms of the second Pauli matrix $\varepsilon \equiv \mathrm{i}\tau^2$, and

$$(H^\dagger \mathrm{i} \overleftrightarrow{D}_\mu H) \equiv H^\dagger (\mathrm{i} D_\mu H) - (\mathrm{i} D_\mu H^\dagger) H;$$
$$(H^\dagger \mathrm{i} \overleftrightarrow{D}_\mu^I H) \equiv H^\dagger \tau^I (\mathrm{i} D_\mu H) - (\mathrm{i} D_\mu H^\dagger) \tau^I H,$$

where τ^I are the Pauli matrices, $T^A \equiv \lambda^A/2$, λ^A are the Gell-Mann matrices, D_μ is the covariant derivative of the SM, and the indices p, r, s, and t take values 1, 2, 3 corresponding to the generation number.

The Warsaw basis operators are divided into eight groups. The first four groups contain operators made of only bosonic fields. Four operators of the first group, X^3, are constructed from field strength tensors and their duals for the SM gauge fields: $G_\mu^{A\nu}$ and $W_\mu^{I\nu}$, $\widetilde{G}_\mu^{A\nu}$ and $\widetilde{W}_\mu^{I\nu}$. The second group, H^6, contains only one operator made of the Higgs field. The third group of operators, $H^4 D^2$, consists of two operators containing Higgs fields, ordinary derivatives, and the SM covariant derivatives. The fourth group of eight operators consists of the Higgs fields, gauge field strength tensors, and their duals. The fifth, $\psi^2 H^3 + \text{h.c.}$, the sixth, $\psi^2 XH$, and the seventh, $\psi^2 H^2 D$, groups respectively contain three, eight, and

eight operators, and consist of fermion and antifermion fields, the Higgs and the conjugate Higgs field, strength tensors, and covariant derivatives of the SM gauge fields. The eighth group is formed by 25 four-fermion operators constructed from the products of left doublets and right singlets of SM fermions with all possible chiral combinations: $(\bar{L}L)(\bar{L}L)$, $(\bar{R}R)(\bar{R}R)$, $(\bar{L}L)(\bar{R}R)$, $(\bar{L}R)(\bar{R}L)+\text{h.c.}$, and $(\bar{L}R)(\bar{L}R)+\text{h.c.}$.

Thus, the Warsaw basis contains $4+1+2+8+3+8+8+25=59$ operators. All conservation laws are assumed to be satisfied, including the lepton and baryon charge conservations, and the minimal mixing is assumed in the quark sector in accordance with the Cabibbo–Kobayashi–Maskawa matrix. If these assumptions are not made, then the basis of dimension-six operators contains 2499 operators in the most general case [15]. Many other versions of the operator basis have also been proposed, but the Warsaw basis is accepted by the scientific community as a common tool for carrying out various calculations and analyzing data from various experiments. The agreement on the choice of a single basis fundamentally allows comparing different results.

We give a small example illustrating the problem of finding an operator basis [16]: the ϕ^4 model described by the Lagrangian

$$\mathcal{L}=\frac{1}{2}(\partial\phi)^2-\frac{\lambda}{4}\phi^4\,. \tag{2}$$

There are three dimension-six operators:

$$\phi^6,\ (\partial^2\phi)^2,\ \phi^2(\partial\phi)^2\,.$$

The question is how many independent operators exist. It turns out that only one of these three operators, say, ϕ^6, is independent. This follows from the equation of motion

$$\partial_\mu\partial^\mu\phi+\lambda\phi^3=0$$

and two relations that are implied by the equation of motion and the fact that, when using integration by parts, the total derivative does not contribute to the action,

$$(\partial^2\phi)^2-\lambda^2\phi^6=(\partial^2\phi-\lambda\phi^3)(\partial^2\phi+\lambda\phi^3)=0\,,$$

given the equation of motion

$$0=\partial_\mu(\phi^3\partial^\mu\phi)=3\phi^2(\partial\phi)^2+\phi^3\partial^2\phi=3\phi^2(\partial\phi)^2-\lambda\phi^6.$$

When finding a basis of independent operators, a natural question arises: why does the derivation rely on the classical equations of motion, which follow only from the SM Lagrangian, or only from Lagrangian (2) in the above simple example, without the order-$1/\Lambda^2$ additions to the equations of motion that follow from the effective Lagrangian? We can imagine that one of the SM equations of motion, for example, relates the covariant derivative and the current:

$$D_\mu F^{\mu\nu}-gj^\nu=0\,.$$

Then, an expression proportional to $1/\Lambda^2$ occurs instead of zero on the left-hand side in the corresponding equation following from Lagrangian (1). If there are two operators that differ from each other only in that one contains $D_\mu F^{\mu\nu}$ and the other contains j^ν, then the difference between their contributions to effective Lagrangian (1) has the next order of smallness, $1/\Lambda^4$, when equations of motion (1) are used in these operators. Therefore, up to the next order of smallness in $1/\Lambda^2$, these operators are equivalent.

4. $1/\Lambda^4$ contributions

One of the serious and widely discussed problems related to the SMEFT formalism is the question: is it necessary to take terms of the order of $1/\Lambda^4$ into account when calculating the contributions to the cross sections and other characteristics of the processes? The cross section of the processes, including the contribution of the SMEFT operators, has the general form

$$\begin{aligned}\sigma_{\text{SMEFT}}=\sigma^{\text{SM}}&+\left(\sum_i\frac{C_i^{(6)}}{\Lambda^2}\,\text{Int}_i^{(\text{SM}\times6)}+\text{h.c.}\right)\\&+\left(\sum_{i,j}\frac{C_i^{(6)}\times C_j^{(6^*)}}{\Lambda^4}\,\sigma_{ij}^{(6\times6^*)}+\text{h.c.}\right)\\&+\left(\sum_j\frac{C_j^{(8)}}{\Lambda^4}\,\text{Int}_i^{(\text{SM}\times8)}+\text{h.c.}\right)+\ldots\,.\end{aligned} \tag{3}$$

As we see from formula (3), an order-$1/\Lambda^2$ term comes from the interference of the contributions of the SMEFT operators with the SM contributions ($\text{Int}_i^{(\text{SM}\times6)}$), while an order-$1/\Lambda^4$ term is given by the squared contribution of the dimension-six SMEFT operators and the interference of the dimension-eight operator contributions with the SM contributions ($\text{Int}_i^{(\text{SM}\times8)}$).

Three possible answers to the question posed about the need to take quadratic contributions of the order of $1/\Lambda^4$ into account can be found in the literature.

(1) Only terms of the order of $1/\Lambda^2$ (i.e., only terms due to interference with the SM contributions) must be kept, because we still cannot take dimension-eight operators into account, and therefore the $1/\Lambda^4$ contributions cannot be properly taken into account.

(2) It is necessary to include not only terms of the order of $1/\Lambda^2$ but also some of the $1/\Lambda^4$ terms that come from the quadratic contributions of dimension-six operators. This is justified by the fact that in some cases the interference terms with SM contributions are equal to zero, for example, for operators describing flavor-changing neutral currents (FCNC), or are very small, for example, contributions to the amplitudes of certain chiralities. Also, without including the quadratic terms, the cross sections can be ill defined: they can be negative when the SM contribution is very small.

(3) The analysis must always be carried out twice: with and without the $1/\Lambda^4$ contributions taken into account. Comparing the results of the two analyses should then make it possible to clarify the applicability range of the approach and thus obtain more reasonable constraints. This standpoint is clearly formulated in [17], and it is this approach that seems to be the most reasonable. In Fig. 4, we show how to extract the bounds on the Wilson coefficients in the SMEFT approach. For this, the idea is to carry out an analysis in the case where only terms of the order $1/\Lambda^2$ are taken into account and in the case where terms of the order $1/\Lambda^4$ are also taken into account, depending on the cutoff from above for some kinematical variable like the total energy $\hat{s}$ of the parton process or the total transverse energy H_{T} of the process. Cutoffs of this type, indicated in the figure as E_{cut}^2, are to ensure the unitarity and guarantee that the computation and analysis exclude ranges where unitary behavior could be

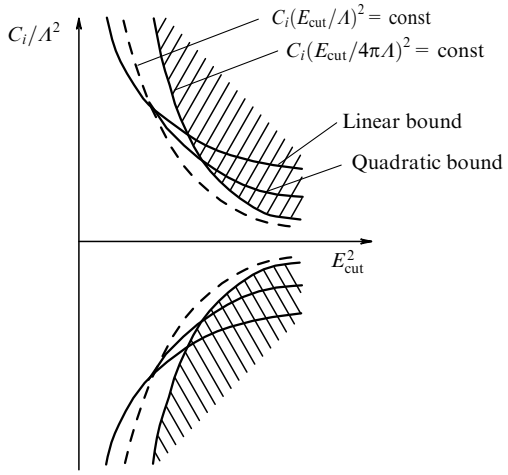

Figure 4. Schematic representation of the procedure for extracting bounds [17] on Wilson coefficients for dimension-six operators in the SMEFT approach.

violated. The regions above the curves in Fig. 4 labeled as $C_i(E_{\text{cut}}/\Lambda)^2 = \text{const}$ and $C_i[E_{\text{cut}}/(4\pi\Lambda)]^2 = \text{const}$ correspond to ranges where either the calculation of the higher corrections fails, which is to be discussed in Sections 5 below, or the perturbative unitarity condition is violated. As a result of the analysis carried out with only linear or with linear and quadratic contributions in $1/\Lambda^2$, kept for different values of the cutoff E_{cut} with the condition restricted to allowed regions, a cutoff is found at which these two methods of analysis yield close constraints on the Wilson coefficient C_i. The constraints thus obtained are the most consistent and do not violate the perturbativity and unitarity conditions.

But it must be borne in mind that the problem is in fact more complex. In a number of cases where unstable particles with subsequently decay are produced, dimension-six operators contribute both to the production process and to the decay process. In such cases, it is necessary to carefully single out the leading and next-to-leading contributions in $1/\Lambda^2$ to squared matrix elements, using the fact that the total width of unstable particles in the corresponding denominators of the amplitudes also contains contributions of dimension-six operators.

A convenient technique for computations and modeling processes with unstable particles, which allows separating linear and quadratic contributions, is the method of auxiliary fields [18]. The main idea of the method is to introduce additional subsidiary vector bosons $\text{V1}_{\text{subsidiary}}$, $\text{V2}_{\text{subsidiary}}$, ... with the same masses and coupling parameters as the gauge bosons in the SM, but with anomalous coupling at the vertex where the anomalous contribution from the dimension-six operator is considered. The introduction of additional vector bosons leads to an increase in the number of Feynman diagrams for the process under consideration. Depending on the requirements for a particular problem, it is possible to turn individual diagrams 'on' and 'off' when calculating matrix elements corresponding to the linear contribution of anomalous operators, the interference terms, and other terms of a higher order in $1/\Lambda^2$. The efficiency of the method is demonstrated via the example of the problem of searching for anomalous operators at the vertex describing the t quark coupling to the W boson and the b quark, including anomalous interactions for all three processes: t-channel, s-channel, and tW (a single t-quark production).

We note that there are cases where expansions only begin with operators of dimension 8, as in models with extra spatial dimensions after integrating out heavy gravitational modes. An example of such an analysis is given in [19].

5. SMEFT and higher-order perturbative corrections

It is well known that, in calculating the characteristics of SM processes, an important role is played by perturbative corrections beyond the leading order (LO) in quantum chromodynamics (QCD): the next-to-leading order (NLO) and the next-to-next-to-leading order (NNLO); in some cases, especially for processes in lepton colliders, electroweak (EW) perturbative corrections in quantum electrodynamics (QED) are also important. Such corrections not only result in significant changes to the cross sections of the processes and, possibly, some kinematical distributions, but also stabilize the results with respect to the variation in the renormalization and factorization scales that arise when calculating higher-order corrections. Therefore, taking the corrections into account increases the accuracy of theoretical predictions, which, in turn, leads to a decrease in process modeling uncertainties in the analysis of experimental data.

In the SMEFT approach, a question naturally arises about the perturbative corrections, first and foremost about the QCD NLO corrections, to the contributions of higher-dimension operators. How is the renormalization procedure implemented in the SMEFT approach? From a naive standpoint, it would seem that it is theoretically impossible to do this consistently, because theories involving operators with dimensions higher than 4 belong to the class of nonrenormalizable theories in terms of the formal power-counting in loop diagrams. But it turns out in this case that the renormalization procedure can be applied to the perturbative SM corrections sequentially in each order in $1/\Lambda^2$. Gauge invariance and the previously noted local nature of the counterterms prove quite helpful here [13, 20]. Gauge invariance guarantees that in each order in $1/\Lambda^2$ the number of operators and corresponding Wilson coefficients is finite, even if quite large. Because the operator basis contains all operators in each order in $1/\Lambda^2$, all counterterms that must preserve gauge invariance and appear in calculating the corrections are again expressed in terms of the operators of the same complete set, which allows the renormalization procedure to be carried out. The situation here is the same as for any running coupling constant in a renormalizable field theory: the Wilson coefficient is measured on some scale, and the theory predicts its value on any other scale. Naturally, all coefficients $C_i^{(6)}$ and the contributions $\text{Int}_i^{(\text{SM}\times 6)}$, $\sigma_{ij}^{(6\times 6^*)}$, etc., in formula (3) become dependent on the renormalization scale μ^2. The renormalization procedure results, generally speaking, in a mixing of the operator contributions. The Wilson coefficients satisfy the renormalization-group equation

$$\mu \frac{\mathrm{d}}{\mathrm{d}\mu} C_i^{(6)}(\mu) = \sum_j \gamma_{ij} C_j^{(6)}(\mu)\,, \tag{4}$$

where γ_{ij} is the matrix of anomalous dimensions, off-diagonal in general. In [15, 21, 22], the full 59×59 matrix of anomalous dimensions for dimension-six operators is given in the one-loop approximation, including not only QCD corrections but also corrections due to Yukawa couplings and the Higgs self-coupling.

Importantly, the contribution of other dimension-six operators — those that did not contribute at the tree level — appears when calculating higher-order corrections. In practice, higher-order calculations in the SMEFT approach are quite complex, and it is therefore not yet possible to fully automate such calculations. But quite a large number of calculations that take higher orders into account have been performed for specific processes involving the production and decay of the Higgs boson or the t quark [23–49].

Several examples are discussed in Sections 6–8 below.

6. SMEFT in the study of Higgs boson couplings

6.1 Higgs boson decay $h \to b\bar{b}$

Calculation of the complete set of NLO corrections for QCD and QED, as well as corrections due to the Yukawa coupling to the Higgs boson decay $h \to b\bar{b}$ [34, 48] in the SMEFT approach, showed that 45 dimension-six operators contribute at that level. In calculating the corrections, it is convenient to introduce the dimensional Wilson coefficients related to the coefficients of the Warsaw basis as $\bar{C}_i = C_i^{(6)}/\Lambda^2$. In many studies, constraints on these parameters are given in units of TeV^{-2}. In the calculations in [48], whose logic we follow here, the set of initial parameters was given by

$$\alpha_s,\ \alpha,\ m_f,\ M_H,\ M_W,\ M_Z,\ V_{ij},\ \bar{C}_i\,.$$

Here, $\alpha_s = g_s^2/(4\pi)$ and $\alpha = e^2/(4\pi)$ are the strong and electromagnetic coupling constants, m_f, M_H, M_W, and M_Z are the fermion, Higgs boson, W-boson, and Z-boson masses, and V_{ij} are the elements of the Cabibbo–Kobayashi–Maskawa mixing matrix. The expression for the decay width is the sum of the leading term, labeled with the superscript (0), and the contribution of the first perturbative correction, labeled with the superscript (1):

$$\Gamma(h \to b\bar{b}) = \Gamma^{(0)} + \Gamma^{(1)}\,.$$

In contrast to the standardly calculated perturbative SM corrections, the SMEFT leading terms and corrections consist of two parts corresponding to operators of dimension four and six:

$$\Gamma^{(0)} = \Gamma^{(4,0)} + \Gamma^{(6,0)}\,,$$
$$\Gamma^{(1)} = \Gamma^{(4,1)} + \Gamma^{(6,1)}\,.$$

The dimension-six contributions come from the interference of the SM contributions and the dimension-six Warsaw-basis operators. Quadratic corrections of the order of $1/\Lambda^4$, which were discussed in Section 5, were not taken into account in this analysis; this problem remains unresolved. The two-particle decay rate, corrected in the first order of the perturbation theory, as is usually the case with perturbative corrections in field theory, is the sum of the tree contribution, the tree level contribution, the interference contribution of tree and loop two-particle amplitudes, and the three-particle tree contribution with the emission of a gluon (strong correction) and a photon (electroweak correction):

$$\Gamma = \int \frac{d\Phi_2}{2M_H}\,|\mathcal{M}_{h\to b\bar{b}}|^2 + \int \frac{d\Phi_3}{2M_H}\,|\mathcal{M}_{h\to b\bar{b}(g,\gamma)}|^2\,,$$

where $d\Phi_i$, $i = 2, 3$, is an element of two- and three-particle phase space. The Kinoshita–Lee–Nauenberg (KLN) theorem [50, 51] guarantees that, when adding the contributions involving the loop correction and the actual gluon or photon emission, the infrared divergences cancel.

An important point to be taken into account is the shift of the SM vacuum expectation value v_{SM} due to the contribution of the operator $O_H = (H^+H)^3$. The potential of the Higgs field H is then expressed as

$$V(H) = \lambda\left(H^\dagger H - \frac{v_{SM}^2}{2}\right)^2 + C_H(H^\dagger H)^3\,.$$

The vacuum expectation value corresponding to the minimum of this potential has the following form under the condition that the correction to the SM potential due to the O_H operator be small:

$$(H^\dagger H)_{min} \equiv \frac{1}{2}\,v_{SMEFT}^2 = \frac{1}{2}\,v_{SM}^2\left(1 - \frac{3\,C_H v_{SM}^2}{4\lambda}\right).$$

In addition, it must be taken into account in calculations that the operators $O_{H\Box} = (H^\dagger H)\Box(H^\dagger H)$ and $O_{HD} = (H^\dagger D_\mu H)^*(H^\dagger D_\mu H)$ lead to the following addition to the Higgs boson field $h(x)$ in the kinetic term,

$$H(x) = \frac{1}{\sqrt{2}}\begin{pmatrix} 0 \\ \left[1 + \left(C_{H\Box} - \frac{1}{4}C_{HD}\right)v_{SM}\right]h(x) + v_{SMEFT} \end{pmatrix},$$

where the Higgs field doublet $H(x)$ is represented in the unitary gauge, and the factor $[1 + (C_{H\Box} - (1/4)C_{HD})v_{SM}]$ must be taken into account in the normalization of $h(x)$ for the kinetic term to be brought to the canonical form.

It must also be borne in mind that the operators O_{HD} and $O_{HWB} = H^\dagger\tau^I H\,W^I_{\mu\nu}B^{\mu\nu}$ contribute to the electroweak coupling constants $g_1 = e/c_W$ and $g_2 = e/s_W$,

$$\bar{g}_1 = g_1\left(1 - \frac{v_{SM}^2}{4}\,C_{HD}\right),$$
$$\bar{g}_2 = g_2\left(1 + v_{SM}^2\,\frac{c_W}{s_W}\left[C_{HWB} + \frac{c_W}{4s_W}\,C_{HD}\right]\right),$$

where s_W and c_W are the sine and cosine of the Weinberg mixing angle.

Thus, the LO contributions to the decay width in the zeroth order (which is the SM contribution) and the first order in $1/\Lambda^2$ take the form

$$\Gamma^{(4,0)} = \frac{N_c m_H m_b^2}{8\pi v_{SM}^2}\,,$$
$$\Gamma^{(6,0)} = 2\Gamma^{(4,0)}\left[C_{H\Box} - \frac{C_{HD}}{4}\left(1 - \frac{c_W^2}{s_W^2}\right) + \frac{c_W}{s_W}\,C_{HWB} - \frac{v_{SM}}{m_b}\,\frac{C_{bH}}{\sqrt{2}}\right]v_{SM}^2\,, \tag{5}$$

where $N_c = 3$ is the number of colors. It can be seen that four Warsaw basis operators contribute to the LO: $O_{H\Box}$, O_{HD}, O_{HWB}, and $O_{bH} = O_{dH}$ for the b-quark, the down quark of the third generation. The operator O_{bH} leads to an addition to the Yukawa SM Lagrangian and hence to an additional contribution to the vertex of the b-quark coupling to the Higgs boson. In formulas (5), the factor β^3, which is close to unity, is omitted, with $\beta = (1 - m_b^2/M_H^2)^{1/2}$.

Calculations of the NLO perturbative corrections themselves are much more laborious compared to calculations of the SM corrections but do not involve any fundamental difference, albeit not without some subtleties in the details of using various renormalization schemes. It is necessary to carefully renormalize all incoming coupling constants, masses, and field functions in the zeroth and first orders in $1/\Lambda^2$. In the $1/\Lambda^2$ order and in the first LO in the coupling constants, new operators appear that also contribute. It turns out that 45 SMEFT operators make a contribution and hence the width depends on 45 Wilson coefficients.

It is well known that, in the minimal subtraction scheme $\overline{\text{MS}}$, some of the QCD corrections reduce to changing the b-quark mass, i.e., to replacing the pole mass $m_\text{b}(m_\text{b})$ with the running mass normalized to the Higgs boson mass M_H, $\overline{m}_\text{b}(M_\text{H})$. The formulas for LO approximation (5) can then be expressed in terms of the mass $\overline{m}_\text{b}(M_\text{H})$ [34, 48]:

$$\overline{\Gamma}^{(4,0)}(M_\text{H}) = \frac{N_\text{c} m_\text{H} \overline{m}_\text{b}^2(M_\text{H})}{8\pi v_\text{SM}^2} \,. \tag{6}$$

Numerically, the value of the running b-quark mass decreases from about 4.8 GeV to 3 GeV when moving to the normalization point M_H, resulting in a noticeable decrease in the partial width $\overline{\Gamma}^{(4,0)}$ compared with $\Gamma^{(4,0)}$ and hence in the leading correction of SMEFT $\overline{\Gamma}^{(6,0)}$ operators compared with $\Gamma^{(6,0)}$.

Results for the LO and NLO contributions can be represented as expressions for $\Delta^\text{LO}(M_\text{H})$ and $\Delta^\text{NLO}(M_\text{H})$ [48] on the scale M_H:

$$\begin{aligned}
\Delta^\text{LO}(M_\text{H}) &\equiv \frac{\overline{\Gamma}^{(4,0)}(M_\text{H}) + \overline{\Gamma}^{(6,0)}(M_\text{H})}{\overline{\Gamma}^{(4,0)}(M_\text{H})} \,, \\
\Delta^\text{NLO}(M_\text{H}) &\equiv \Delta^\text{LO}(M_\text{H}) + \frac{\overline{\Gamma}^{(4,1)}(M_\text{H}) + \overline{\Gamma}^{(6,1)}(M_\text{H})}{\overline{\Gamma}^{(4,0)}(M_\text{H})} \,.
\end{aligned} \tag{7}$$

Nonfactorizable QCD–QED corrections, corrections due to the large Yukawa coupling constant of the t-quark and the Higgs boson, the renormalization of all electroweak constants to the scale M_H, and a number of other, less significant, corrections were taken into account in numerical calculations. The main NLO corrections are related to the contributions of operators that already appear in the LO. The calculation results are given by the following formulas [48]:

$$\begin{aligned}
\Delta^\text{LO}(m_\text{H}) = 1 + \frac{v_\text{SM}^2}{\Lambda^2} \Big[& 3.74 C_{HWB} + 2.00 C_{H\Box} \\
& - 1.41 \, \frac{v_\text{SM}}{\overline{m}_\text{b}} \, C_{bH} + 1.24 C_{HD} \Big] \,,
\end{aligned} \tag{8}$$

$$\begin{aligned}
\Delta^\text{NLO}(m_\text{H}) = 1.13 + \frac{v_\text{SM}^2}{\Lambda^2} \Big[& 4.16 C_{HWB} + 2.40 C_{H\Box} \\
& - 1.73 \, \frac{v_\text{SM}}{\overline{m}_\text{b}} \, C_{bH} + 1.33 C_{HD} \Big] + \dots \,.
\end{aligned} \tag{9}$$

A comparison of formulas (8) and (9) shows that the NLO correction to the SM is 13%. This 13% is made up of about 18% due to QCD–QED NLO corrections and −5% due to other contributions [48]. The correction to the Wilson coefficient C_{HWB} is approximately 11% ($[(4.16 - 3.74)/3.74] \times 100\%$). NLO corrections to the Wilson coefficients $C_{H\Box}$, C_{bH}, and C_{HD} are close to 20%, 23%, and 7%, respectively. The corrections are significant and must be taken into account when imposing experimental bounds.

6.2 Higgs boson decay $\text{h} \to \gamma\gamma$

The SMEFT NLO corrections in QCD for the $\text{h} \to \gamma\gamma$ decay were calculated in [29, 30, 43] within two independent approaches. In the approach in [43], the correction is presented in terms of the ratio of the Higgs boson decay width into two photons, taking into account the contribution of the NLO operators and corrections to the SM width of this decay,

$$\mathcal{R}_{\text{h}\to\gamma\gamma} = \frac{\Gamma(\text{SMEFT}, \text{h} \to \gamma\gamma)}{\Gamma(\text{SM}, \text{h} \to \gamma\gamma)} \equiv 1 + \delta\mathcal{R}_{\text{h}\to\gamma\gamma} \,,$$

where the SM width is given by a well-known formula [62–64] in which only the leading contribution of the t quark is kept among all fermion contributions to the triangular loop,

$$\begin{aligned}
&\Gamma(\text{SM}, \text{h} \to \gamma\gamma) = \frac{G_\text{F} \alpha_\text{EM}^2 M_\text{H}^3}{128\sqrt{2}\pi^3} \, |I_{\gamma\gamma}|^2 \,, \\
&I_{\gamma\gamma} \equiv I_{\gamma\gamma}(r_\text{t}, r_\text{W}) = Q_\text{t}^2 N_\text{c} A_{1/2}(r_\text{t}) - A_1(r_\text{W}) \,, \\
&A_{1/2}(r_\text{t}) = 2 r_\text{t} \big[1 + (1 - r_\text{t}) f(r_\text{t}) \big] \,, \\
&A_1(r_\text{W}) = 2 + 3 r_\text{W} \big[1 + (2 - r_\text{W}) f(r_\text{W}) \big] \,.
\end{aligned}$$

Here, Q_t and m_t are the t-quark charge and mass, $N_\text{c} = 3$, $r_\text{t} \equiv 4m_\text{t}^2/M_\text{H}^2$, $r_\text{W} \equiv 4M_\text{W}^2/M_\text{H}^2$, and the function $f(r)$ is finite and can be represented in the form

$$f(r) = \begin{cases} \arcsin^2 \left(\dfrac{1}{\sqrt{r}} \right) , & r \geqslant 1 \,, \\ -\dfrac{1}{4} \left[\log \left(\dfrac{1 + \sqrt{1 - r}}{1 - \sqrt{1 - r}} \right) - \text{i}\pi \right]^2 , & r \leqslant 1 \,. \end{cases}$$

We note that the three Warsaw-basis operators

$$\begin{aligned}
&O_{HW} = H^\dagger H \, W^I_{\mu\nu} W^{I\mu\nu} \,, \quad O_{HB} = H^\dagger H \, B_{\mu\nu} B^{\mu\nu} \,, \\
&O_{HWB} = H^\dagger \tau^I H \, W^I_{\mu\nu} B^{\mu\nu}
\end{aligned}$$

contribute at the tree level to the vertex of the Higgs boson coupling with two photons after the Higgs field acquires a vacuum expectation value and spontaneous symmetry breaking occurs. Exactly these operators determine the dominant part of the correction to the SM contribution and of the NLO corrections. The operators

$$O_{uW} = (\bar{q}_p \sigma^{\mu\nu} u_r) \tau^I \tilde{H} \, W^I_{\mu\nu} \,, \quad O_{uB} = (\bar{q}_p \sigma^{\mu\nu} u_r) \tilde{H} \, B_{\mu\nu}$$

for the top quark of the third generation ($u = t$) lead to the appearance of a four-point interaction vertex $\bar{\text{t}}\text{t}\text{h}\gamma$. Such a vertex contributes via the t-quark loop to the $\text{h} \to \gamma\gamma$ decay process. The corresponding contributions, proportional to the inverse scale $1/\Lambda^2$ and the Wilson coefficients, are also added to the SM contribution, but are numerically much smaller. The calculation result can be represented by the following formula, which explicitly shows the dependence on the normalization scale μ^2 [43]:

$$\begin{aligned}
\delta\mathcal{R}_{\text{h}\to\gamma\gamma} \simeq & - \left[48.04 - 1.07 \log \frac{\mu^2}{M_\text{W}^2} \right] C^{HB} \\
& - \left[14.29 - 0.12 \log \frac{\mu^2}{M_\text{W}^2} \right] C^{HW} \\
& + \left[26.62 - 0.52 \log \frac{\mu^2}{M_\text{W}^2} \right] C^{HWB}
\end{aligned}$$

$$+\left[2.11-0.84\log\frac{\mu^2}{M_{\rm W}^2}\right]C^{tB}$$
$$+\left[1.13-0.45\log\frac{\mu^2}{M_{\rm W}^2}\right]C^{tW}+\ldots\,.$$

Several other operators contribute to the width of the Higgs boson decay into two photons [43], but numerically these contributions are negligible. The QCD NLO corrections to these contributions are of the order of 10%. The operators O_{uB} and O_{uW} start making a contribution only at the loop level, and this contribution is much less significant. Data on the signal strength or the Higgs boson decay into two photons at the LHC allow obtaining bounds only on the above five Wilson coefficients [43]:

$$|C^{HB}|\lesssim\frac{0.003}{(1\ {\rm TeV})^2}\,,\quad |C^{HW}|\lesssim\frac{0.011}{(1\ {\rm TeV})^2}\,,\quad |C^{HWB}|\lesssim\frac{0.006}{(1\ {\rm TeV})^2}\,,$$
$$|C^{tB}|\lesssim\frac{0.071}{(1\ {\rm TeV})^2}\,,\quad |C^{tW}|\lesssim\frac{0.133}{(1\ {\rm TeV})^2}\,. \qquad (10)$$

We note that operator C^{HWB} makes a direct contribution [52] to the Peskin–Takeuchi S parameter [53]:

$$C^{HWB}=\frac{G_{\rm F}\,\alpha_{\rm EM}}{2\sqrt{2}sc}\,\Delta S\,.$$

Data on precision measurements of the electroweak parameters at the Z-boson pole give bounds on the parameter S [54], $\Delta S\in[-0.06,\,0.07]$, which leads to a constraint on the Wilson coefficient C^{HWB},

$$|C^{HWB}|\lesssim 0.005\ {\rm TeV}^{-2}\,,$$

which practically coincides with constraints (10) [43] deduced from the Higgs boson signal strength. The constraints on the coefficients $|C^{HB}|$ and $|C^{HW}|$ obtained in [54, 55] from the LHC data and precision measurements of electroweak parameters are in good agreement with constraints (10). At the same time, the constraints on the Wilson coefficients $|C^{tB}|$ and $|C^{tW}|$ given in (10) are approximately an order of magnitude more stringent than those following from the analysis of the $\bar{\rm t}{\rm t}{\rm Z}$ process: $|C^{tB}|\lesssim 7.1\ {\rm TeV}^{-2}$ and $|C^{tW}|\lesssim 2.5\ {\rm TeV}^{-2}$ [61].

The above example illustrates one of the advantages of the SMEFT approach: the ability to consistently compare the results deduced from the data of essentially different experiments.

6.3 SMEFT and the κ formalism

When analyzing deviations from SM predictions in processes involving the Higgs boson, the so-called κ formalism is often used in theoretical and experimental studies [56, 57]. In this formalism, the terms of the SM Lagrangian are multiplied by the factors κ_i, which are called modifiers of the Higgs boson coupling constants, and the Lagrangian itself is written as

$$\mathcal{L}_\kappa=\kappa_{\rm W}2m_{\rm W}^2W_\mu^+W^{-\mu}\,\frac{h}{v_{\rm SM}}+\kappa_Z m_{\rm Z}^2Z_\mu Z^\mu\,\frac{h}{v_{\rm SM}}$$
$$-\sum_\psi\kappa_\psi m_\psi\bar\psi\psi\,\frac{h}{v_{\rm SM}}+\frac{g_{\rm s}^2}{32\pi^2}\,\kappa_g G^a_{\mu\nu}G^{a\mu\nu}\,\frac{h}{v_{\rm SM}}$$
$$+\frac{e^2}{16\pi^2}\,\kappa_\gamma F_{\mu\nu}F^{\mu\nu}\,\frac{h}{v_{\rm SM}}+\frac{e^2}{16\pi^2}\,\kappa_{Z\gamma}Z_{\mu\nu}F^{\mu\nu}\,\frac{h}{v_{\rm SM}}\,, \qquad (11)$$

where the symbol ψ denotes all fermions of the SM. Obviously, for $\kappa_{\rm W}$, $\kappa_{\rm Z}$, and κ_ψ equal to unity and $\kappa_{\rm g}$, κ_γ, and $\kappa_{{\rm Z}\gamma}$ equal to zero, Lagrangian (11) becomes the tree Lagrangian of the SM. In the SM, the terms in (11) proportional to $\kappa_{\rm g}$, κ_γ, or $\kappa_{{\rm Z}\gamma}$ arise at the loop level, and these coefficients themselves are expressed via well-known formulas like (10) in terms of the SM parameters (coupling constants and the t-quark, W-boson, and Higgs-boson masses), as well as in terms of the modifiers $\kappa_{\rm W}$, $\kappa_{\rm Z}$, and $\kappa_{\rm t}$.

In experiments, the bounds for modifiers are determined from measurements of the cross sections and decay widths in accordance with the obvious formulas

$$\kappa_i^2=\frac{\sigma_i}{\sigma_i^{\rm SM}}\ \ \text{or}\ \ \kappa_i^2=\frac{\Gamma^i}{\Gamma^i_{\rm SM}}\,. \qquad (12)$$

Figure 5 shows the results for the allowed spread in the values of modifiers of the Higgs boson coupling constants obtained from analyzing the LHC data at an energy of 13 TeV by the ATLAS collaboration (Fig. 5a) [58] and the CMS collaboration (Fig. 5b) [59], as well as the expected accuracy in determining these modifiers, which can be obtained at the LHC in the high-luminosity regime of 3 ab^{-1} at a 14-TeV collision energy (Fig. 5c) [57].

We note, however, that the κ formalism is not gauge invariant with respect to the SM electroweak group. In this formalism, it is impossible to calculate the perturbative corrections consistently, which leads to significant theoretical uncertainties in predictions and therefore affects the accuracy of process modeling in the analysis of experimental data. These circumstances motivate the LHC experimental collaborations to analyze data using the SMEFT approach, which is more consistent than the κ formalism.[1] The analysis is based on calculations of perturbative corrections done in the SMEFT formalism, which we briefly discussed above. Using the full collected statistics, the CMS collaboration analyzed data both in the κ formalism and in the SMEFT approach. Preliminary results are shown in Fig. 6 [60]. As can be seen, different signs of the coefficients are still not ruled out in a number of cases, either in the κ formalism or in the SMEFT, and the accuracy of the constraints is not high in many cases. Therefore, many possibilities remain for manifestations of various extensions of the SM and the allowed parameter regions of the corresponding models.

[1] Let us clarify that, as long as we are talking about imposing bounds on the κ parameters with ever-increasing precision, the κ formalism is not fraught with any particular problems. But if some deviation starts appearing, then the question of the significance of this deviation becomes very acute. In this case, a question naturally arises about the accuracy of the deviation modeling and hence the question about the theoretical uncertainty as part of the systematic error in the analysis. These issues inevitably call into question the proof of the statistical significance of the deviation in the κ formalism, which would then require more reasonable signal modeling based on a more theoretically consistent gauge-invariant formalism, such as the SMEFT. Therefore, the CMS and ATLAS collaborations are already increasingly reliant on the SMEFT formalism to model deviations and impose bounds. If a significant deviation is found in some Wilson coefficients divided by Λ^2, then it is necessary to conduct a detailed analysis of various models leading to precisely those operators in whose coefficients the deviations are found. Comparing the details of the predictions of different models, it would then be possible to single out those that are more likely to describe the deviations. We return to this discussion in Section 9.

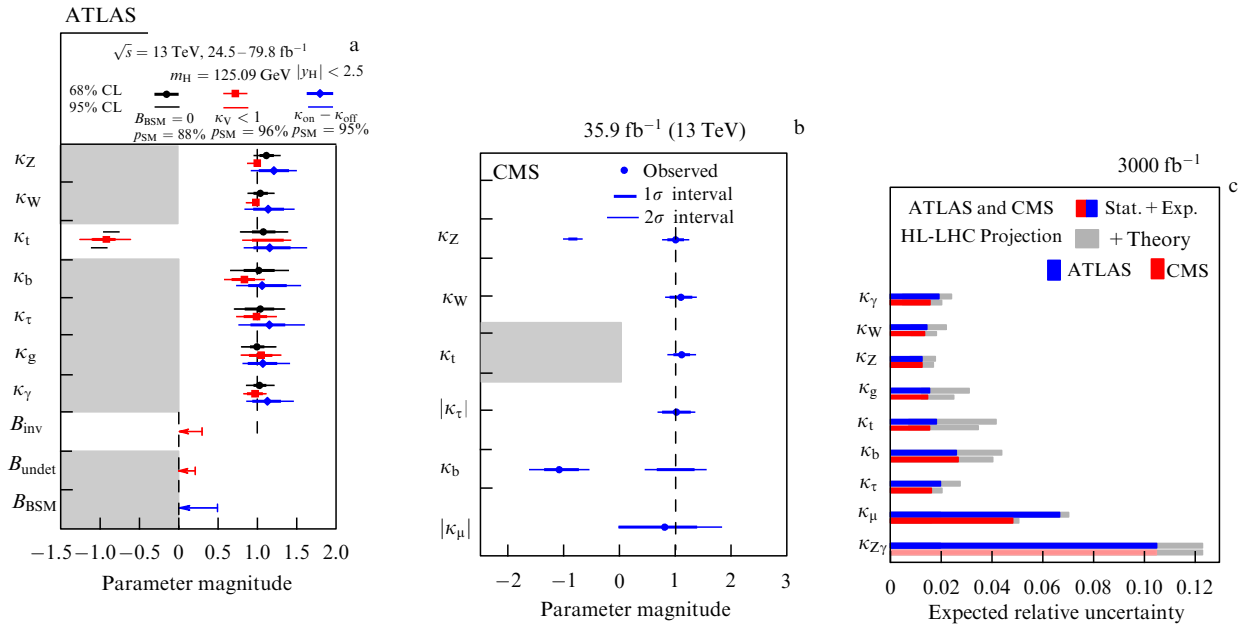

Figure 5. (Color online.) Modifiers of Higgs boson coupling constants from LHC data at 13 TeV: (a) ATLAS [58] and (b) CMS [59]. (c) Modifiers expected at the LHC in the high-luminosity regime of 3 ab^{-1} at an energy of 14 TeV [57].

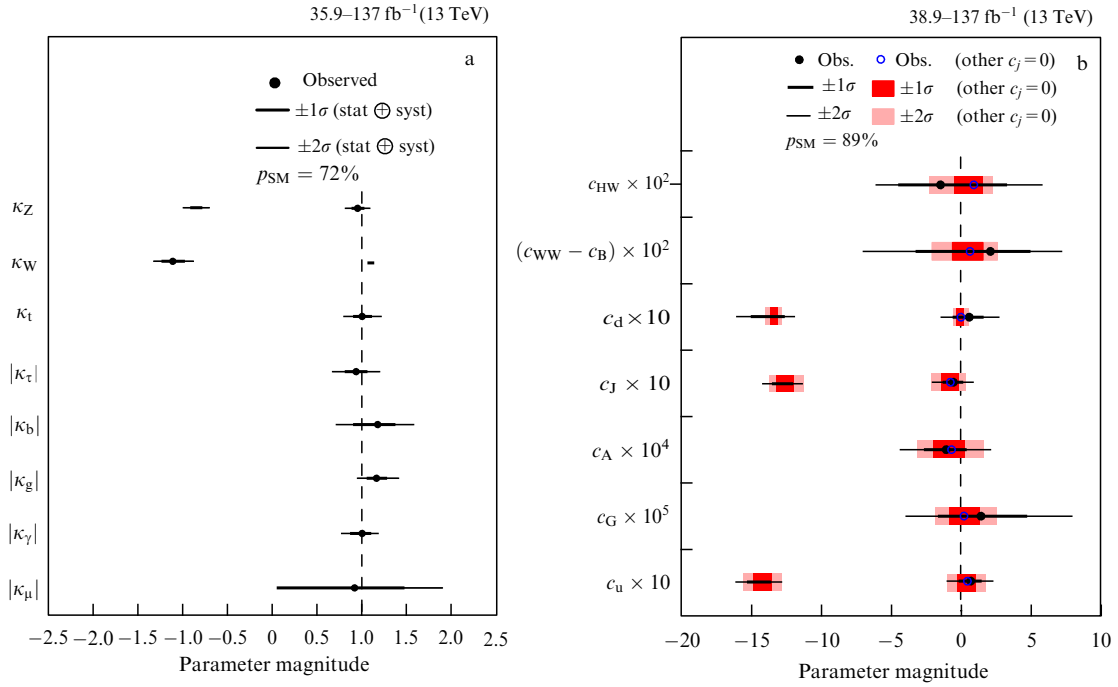

Figure 6. (Color online.) Preliminary CMS collaboration results [60] on measuring modifiers κ of (a) Higgs boson coupling constants and (b) constraints on the Wilson coefficients for a number of SMEFT operators from LHC data at 13 TeV, based on statistics up to 137 fb^{-1} [60].

7. t-quark sector in the SMEFT approach

The 28 Warsaw-basis operators directly enter the t-quark sector. This set includes 9 operators made of two quark and two bosonic fields, 11 four-quark operators, and 8 operators made of two quark and two lepton fields. In addition to these operators, which preserve the baryon and lepton quantum numbers, there are five more operators that violate them. The explicit form of all these operators in exact correspondence with the original notation for the Warsaw basis is presented in Table 2 and in a somewhat different notation in [17].

Twenty-eight operators containing at least one t-quark field are listed in Table 2. They do not include operators of the first four groups of Warsaw-basis operators, include one operator from the fifth group, four operators of the sixth and seventh groups, and 19 four-fermion operators from the eighth group with fermions of the left (L) and right (R) chiralities in all possible combinations. The operators in Table 2 preserve the lepton and baryon quantum numbers. There are five more dimension-six operators [14, 17] that violate the lepton and baryon quantum numbers. We do not present their explicit form.

Table 2. Twenty-eight operators of dimension 6 from the complete set of 59 Warsaw basis operators containing the t quark and contributing to processes involving it.

$5:\psi^2H^3+\text{h.c.}$	
O_{uH}	$(H^\dagger H)(\bar{q}_p u_r \tilde{H})$

$6:\psi^2XH+\text{h.c.}$		$7:\psi^2H^2D$	
O_{uG}	$(\bar{q}_p\sigma^{\mu\nu}T^A u_r)\tilde{H}G^A_{\mu\nu}$	$O^{(1)}_{Hq}$	$(H^\dagger \mathrm{i}\overleftrightarrow{D}_\mu H)(\bar{q}_p\gamma^\mu q_r)$
O_{uW}	$(\bar{q}_p\sigma^{\mu\nu}u_r)\tau^I\tilde{H}W^I_{\mu\nu}$	$O^{(3)}_{Hq}$	$(H^\dagger \mathrm{i}\overleftrightarrow{D}^I_\mu H)(\bar{q}_p\tau^I\gamma^\mu q_r)$
O_{uB}	$(\bar{q}_p\sigma^{\mu\nu}u_r)\tilde{H}B_{\mu\nu}$	O_{Hu}	$(H^\dagger \mathrm{i}\overleftrightarrow{D}_\mu H)(\bar{u}_p\gamma^\mu u_r)$
O_{dW}	$(\bar{q}_p\sigma^{\mu\nu}d_r)\tau^I H W^I_{\mu\nu}$	$O_{Hud}+\text{h.c.}$	$\mathrm{i}(\tilde{H}^\dagger D_\mu H)(\bar{u}_p\gamma^\mu d_r)$

$8:(\bar{\mathrm{L}}\bar{\mathrm{L}})(\bar{\mathrm{L}}\bar{\mathrm{L}})$		$8:(\bar{\mathrm{R}}\bar{\mathrm{R}})(\bar{\mathrm{R}}\bar{\mathrm{R}})$		$8:(\bar{\mathrm{L}}\bar{\mathrm{L}})(\bar{\mathrm{R}}\bar{\mathrm{R}})$	
$O^{(1)}_{qq}$	$(\bar{q}_p\gamma_\mu q_r)(\bar{q}_s\gamma^\mu q_t)$	O_{uu}	$(\bar{u}_p\gamma_\mu u_r)(\bar{u}_s\gamma^\mu u_t)$	O_{lu}	$(\bar{l}_p\gamma_\mu l_r)(\bar{u}_s\gamma^\mu u_t)$
$O^{(3)}_{qq}$	$(\bar{q}_p\gamma_\mu\tau^I q_r)(\bar{q}_s\gamma^\mu\tau^I q_t)$	O_{eu}	$(\bar{e}_p\gamma_\mu e_r)(\bar{u}_s\gamma^\mu u_t)$	O_{qe}	$(\bar{q}_p\gamma_\mu q_r)(\bar{e}_s\gamma^\mu e_t)$
$O^{(1)}_{lq}$	$(\bar{l}_p\gamma_\mu l_r)(\bar{q}_s\gamma^\mu q_t)$	$O^{(1)}_{ud}$	$(\bar{u}_p\gamma_\mu u_r)(\bar{d}_s\gamma^\mu d_t)$	$O^{(1)}_{qu}$	$(\bar{q}_p\gamma_\mu q_r)(\bar{u}_s\gamma^\mu u_t)$
$O^{(3)}_{lq}$	$(\bar{l}_p\gamma_\mu\tau^I l_r)(\bar{q}_s\gamma^\mu\tau^I q_t)$	$O^{(8)}_{ud}$	$(\bar{u}_p\gamma_\mu T^A u_r)(\bar{d}_s\gamma^\mu T^A d_t)$	$O^{(8)}_{qu}$	$(\bar{q}_p\gamma_\mu T^A q_r)(\bar{u}_s\gamma^\mu T^A u_t)$
				$O^{(1)}_{qd}$	$(\bar{q}_p\gamma_\mu q_r)(\bar{d}_s\gamma^\mu d_t)$
				$O^{(8)}_{qd}$	$(\bar{q}_p\gamma_\mu T^A q_r)(\bar{d}_s\gamma^\mu T^A d_t)$

$8:(\bar{\mathrm{L}}\bar{\mathrm{R}})(\bar{\mathrm{R}}\bar{\mathrm{L}})+\text{h.c.}$		$8:(\bar{\mathrm{L}}\bar{\mathrm{R}})(\bar{\mathrm{L}}\bar{\mathrm{R}})+\text{h.c.}$	
O_{ledq}	$(\bar{l}^j_p e_r)(\bar{d}_s q_{tj})$	$O^{(1)}_{quqd}$	$(\bar{q}^j_p u_r)\epsilon_{jk}(\bar{q}^k_s d_t)$
		$O^{(8)}_{quqd}$	$(\bar{q}^j_p T^A u_r)\epsilon_{jk}(\bar{q}^k_s T^A d_t)$
		$O^{(1)}_{lequ}$	$(\bar{l}^j_p e_r)\epsilon_{jk}(\bar{q}^k_s u_t)$
		$O^{(3)}_{lequ}$	$(\bar{l}^j_p\sigma_{\mu\nu}e_r)\epsilon_{jk}(\bar{q}^k_s\sigma^{\mu\nu}u_t)$

The study of possible deviations from the SM in t-quark couplings, which are parameterized by the above operators in the SMEFT approach, and the search for the corresponding experimental manifestations of these deviations are of great scientific interest, largely motivated by the fact that the t-quark is the heaviest among the known elementary particles, with a mass of the order of the vacuum expectation value of the Higgs field, i.e., of the order of the electroweak energy scale. As is well established theoretically and confirmed experimentally, the t quark cannot form strongly bound states (hadrons) because its lifetime is so short compared to the characteristic formation times of hadrons that it decays long before it can bind into colorless hadrons with other quarks or antiquarks. This property allows studying the fundamental structure of t-quark couplings without the influence of hadronization effects. In view of the large mass of the t-quark and rather weak mixing with quarks of the first two generations, it is quite possible that deviations from the SM, parameterized by higher-order operators, can manifest themselves in the sectors of the t quark and the Higgs boson, whose masses, referred to as natural, are of the order of the electroweak scale.

We consider several examples of studying deviations from the SM in t-quark couplings.

7.1 Anomalous Wtb couplings

The coupling of the t quark to the W boson and the b quark, determined by the Wtb vertex, is responsible for the t-quark decay. In the SM, this vertex has the same V–A structure as the other SM vertices in terms of which charged currents are expressed. But many extensions of the SM predict possible changes in the structure of this coupling. The Wtb coupling is studied experimentally at the LHC either directly in the decay of a t quark during its pair production via strong QCD interactions or in a single production event due to electroweak interactions. The single production cross section is proportional to the Wtb vertex squared.

In studying the possible structures of the Wtb vertex, the effective Lagrangian is traditionally used in the form [65]

$$\mathcal{L} = -\frac{g}{\sqrt{2}}\,\bar{b}\gamma^\mu\left(f_{\mathrm{LV}}P_{\mathrm{L}} + f_{\mathrm{RV}}P_{\mathrm{R}}\right)tW^-_\mu - \frac{g}{\sqrt{2}}\,\bar{b}\,\frac{\mathrm{i}\sigma^{\mu\nu}}{2M_{\mathrm{W}}}\left(f_{\mathrm{LT}}P_{\mathrm{L}} + f_{\mathrm{RT}}P_{\mathrm{R}}\right)tW^-_{\mu\nu} + \text{h.c.}\,, \tag{13}$$

where $P_{\mathrm{L,R}} = (1 \mp \gamma_5)/2$ are the projection operators on the left- and right-chiral states, $W^-_{\mu\nu} = \partial_\mu W^-_\nu - \partial_\nu W^-_\mu$, g is the SM electroweak constant for the gauge group $\mathrm{SU_L}(2)$, and $f_{\mathrm{LV(T)}}$ and $f_{\mathrm{RV(T)}}$ are dimensionless coefficients. In particular, the ATLAS and CMS collaborations analyzed the Wtb vertex using Lagrangian (13) so as to impose constraints on the parameters of the anomalous coupling constants. The most stringent constraints on anomalous parameters in the first run of the LHC were obtained in [71]. In finding these constraints, the essential points were the modeling of signal processes and the preparation of a minimum set of event samples by the above method, with subsidiary vector fields introduced that have the same coupling as the SM gauge fields, except for the interaction vertex with an anomalous parameter [18].

The Lorentz structures of Lagrangian (13) [65], which is widely used in the analysis of experimental data and contains anomalous constants of the t-quark coupling to the b quark and the W boson, follow from the four Warsaw basis operators containing the t quark (2): $O_{Hq}^{(3)}$, O_{Hu}, O_{dW}, and O_{uW} [66–69], which are related to the notation in [17] as

$$O_{Hq}^{(3)} \equiv O_{\phi q}^{(3,33)}\,,\ O_{Hu} \equiv O_{\phi ud}^{(33)}\,,\ O_{dW} \equiv O_{dW}^{(33)}\,,\ O_{uW} \equiv O_{uW}^{(33)}\,.$$

The operators $O_{\phi q}^{(3,33)}$, $O_{\phi ud}^{(33)}$, $O_{dW}^{(33)}$, and $O_{uW}^{(33)}$ have the following form in the notation used in [17]:

$$\begin{aligned}
O_{\phi q}^{(3,33)} &= \frac{\mathrm{i}}{2}\left[\phi^\dagger \tau^I (D_\mu \phi) - (D_\mu \phi^\dagger)\tau^I \phi\right](\bar{q}_{\mathrm{L}3}\gamma^\mu \tau^I q_{\mathrm{L}3})\,,\\
O_{\phi ud}^{(33)} &= \mathrm{i}(\tilde{\phi}^\dagger D_\mu \phi)(\bar{t}_{\mathrm{R}}\gamma^\mu b_{\mathrm{R}})\,,\\
O_{dW}^{(33)} &= (\bar{q}_{\mathrm{L}3}\sigma^{\mu\nu}\tau^I b_{\mathrm{R}})\phi\, W_{\mu\nu}^I\,,\\
O_{uW}^{(33)} &= (\bar{q}_{\mathrm{L}3}\sigma^{\mu\nu}\tau^I t_{\mathrm{R}})\tilde{\phi}\, W_{\mu\nu}^I\,,
\end{aligned} \tag{14}$$

where the Higgs field doublet H is denoted by ϕ, $q_{\mathrm{L}3}$ is the left chiral doublet t_{L} and b_{L} of quark fields of the third generation, and t_{R} and b_{R} are the corresponding right chiral fields.

In the relevant notation, the Wilson coefficients $C_{\phi q}^{(3,33)}$, $C_{\phi ud}^{(33)}$, $C_{dW}^{(33)}$, and $C_{uW}^{(33)}$ standing at the operators are related to the anomalous parameters in the Wtb vertex as [66–70]

$$\begin{aligned}
f_{\mathrm{LV}} &= V_{tb} + C_{\phi q}^{(3,33)}\,\frac{v^2}{\Lambda^2}\,,\quad f_{\mathrm{RV}} = \frac{1}{2}\,C_{\phi ud}^{(33)}\,\frac{v^2}{\Lambda^2}\,,\\
f_{\mathrm{LT}} &= \sqrt{2}\,C_{dW}^{(33)}\,\frac{v^2}{\Lambda^2}\,,\quad f_{\mathrm{RT}} = \sqrt{2}\,C_{uW}^{(33)}\,\frac{v^2}{\Lambda^2}\,,
\end{aligned} \tag{15}$$

as can be easily verified from the explicit form of operators (14) in the unitary gauge using the expressions for the Pauli matrices, doublets of the left quark fields, and the Higgs boson.

Compared to the approach in which deviations from the SM are parameterized by anomalous coupling constants that modify the corresponding vertices of the t-quark coupling to other fields, additional point-like vertices with four or five external lines appear in the SMEFT approach. These vertices ensure gauge invariance with respect to the entire SM gauge group. It follows from the form of operators (14) that, in addition to anomalous contributions to the Wtb vertex, additional point four-particle vertices arise, such as Wtbγ, WtbZ, WtbH, $\mathrm{W^+W^-b\bar{b}}$, and five-particle vertices, including Wtbγ H and WtbZH.

An analysis of a single t-quark production in the t-channel in the SMEFT formalism at the NLO level, with the emerging nonresonance contributions from the vertex $\mathrm{W^+W^-b\bar{b}}$ taken into account, showed that, in addition to the appearance of the K factor, the angular distributions of produced particles are somewhat modified [49]. However, these modifications are not significant, at the level of a few percent. But the corrections due to terms of the order of $1/\Lambda^4$ can reach 20% of the order-$1/\Lambda^2$ contributions, which is very significant. A corresponding experimental analysis at the NLO level has not yet been done, but the terms quadratic in anomalous constants, corresponding to the order $1/\Lambda^4$, were taken into account in the ATLAS and CMS experiments, including in the analysis in [71].

7.2 Deviations in t-quark couplings in gluon–gluon collisions

Pair production is the leading t-quark production process at the LHC, with approximately 85% of the production cross sections being due to the contribution of a subprocess with initial-state gluons. In the SM, the cross section and other characteristics are well known and agree with measurements within the accuracy. The cross pair production section, including the NNLO corrections of strong interactions and the NLO corrections of electroweak interactions at a collision energy of 13 TeV, is $\sigma_{\mathrm{SM}}^{\mathrm{t\bar{t}}} = 832^{+20}_{-29}(\mathrm{scales}) \pm 35(\mathrm{PDF}+\alpha_{\mathrm{s}})$ pb [72, 73] (PDF is the probability density function). But, as is well known, taking the t-quark decay into a W-boson and a b-quark into account gives rise to single-resonance and nonresonance contributions appearing in the complete set of diagrams along with the double-resonance contributions of pair production and decays of t-quarks. For the single-resonance contribution corresponding to the $\mathrm{gg} \to \mathrm{tWb}$ process, large QCD corrections to the vertex with the gluon splitting into a $\mathrm{b\bar{b}}$ pair must be taken into account. Resummation of these corrections amounts to the introduction of a distribution function of the b-quark in the proton, and the process of a single production of the t-quark becomes $\mathrm{gb} \to \mathrm{tW}$. We do not discuss the well-known problem of how different contributions should be brought together in order to avoid double counting, but we note that the NNLO corrections to $\mathrm{gb} \to \mathrm{tW}$ are known and the cross section of a single t-quark production process in the mode of associative production with a W boson at the LHC at an energy of 13 TeV is $\sigma_{\mathrm{SM}}^{\mathrm{tW}} = 71.7 \pm 1.8(\mathrm{scales}) \pm 3.4(\mathrm{PDF}+\alpha_{\mathrm{s}})$ pb [74].

Figure 7a,b [75] shows the SM diagrams that make the leading tree-level contribution to the processes of single, $\mathrm{gb} \to \mathrm{tW}$, and pair, $\mathrm{gg} \to \mathrm{t\bar{t}}$, t-quark production. From the form of the vertices included in the process diagrams, it is clear which Warsaw basis operators modify them and produce additional contributions. Thus, in the process of pair production in the SM, the t-quark–gluon interaction vertices $\mathrm{t\bar{t}g}$ and the three-gluon ggg vertex appear. Accordingly, the following operators make a contribution:

$$\begin{aligned}
O_{uG} &= (\bar{q}_p \sigma^{\mu\nu} T^A u_r)\widetilde{H}\, G_{\mu\nu}^A\,,\\
O_G &= f^{ABC} G_\mu^{A\nu} G_\nu^{B\rho} G_\rho^{C\mu}\,,
\end{aligned} \tag{16}$$

where $q_p \equiv q_{\mathrm{L}3}$ and $u_r \equiv t_{\mathrm{R}}$ are the left doublet and right singlet of third-generation quarks ($p = q = 3$). The first operator in (16) is denoted as $O_{uG} \equiv O_{uG}^{33}$ in [17] and as $O_{uG} \equiv O_{tG}$ in [75], with the corresponding notation for the Wilson coefficients in the operators. We note that operator O_{tG} not only leads to an addition to the vertex $\mathrm{t\bar{t}g}$ but also gives rise to a new four-point vertex $\mathrm{t\bar{t}gg}$. Operator O_G, similarly, not only adds to the three-gluon vertex but also gives rise to four-, five-, and six-gluon vertices, which do not contribute to the tree process, but must be taken into account when calculating higher-order corrections. In Fig. 7d, we show the corresponding diagrams and highlight the vertices with the contributions of the SMEFT operators.

We also note that, for indices corresponding to different generations, operator O_{uG} is denoted as O_{uG}^{13} and O_{uG}^{23} in [17] and as $O_{u(c)G}$ in [75]; it adds new flavor-breaking vertices $\mathrm{u\bar{t}g}$ and $\mathrm{c\bar{t}g}$. These operators contribute to the associative tW production process, as is shown in Fig. 7c.

Vertices $\mathrm{t\bar{t}g}$ and Wtb participate in the diagrams of a single t-quark production process in association with the

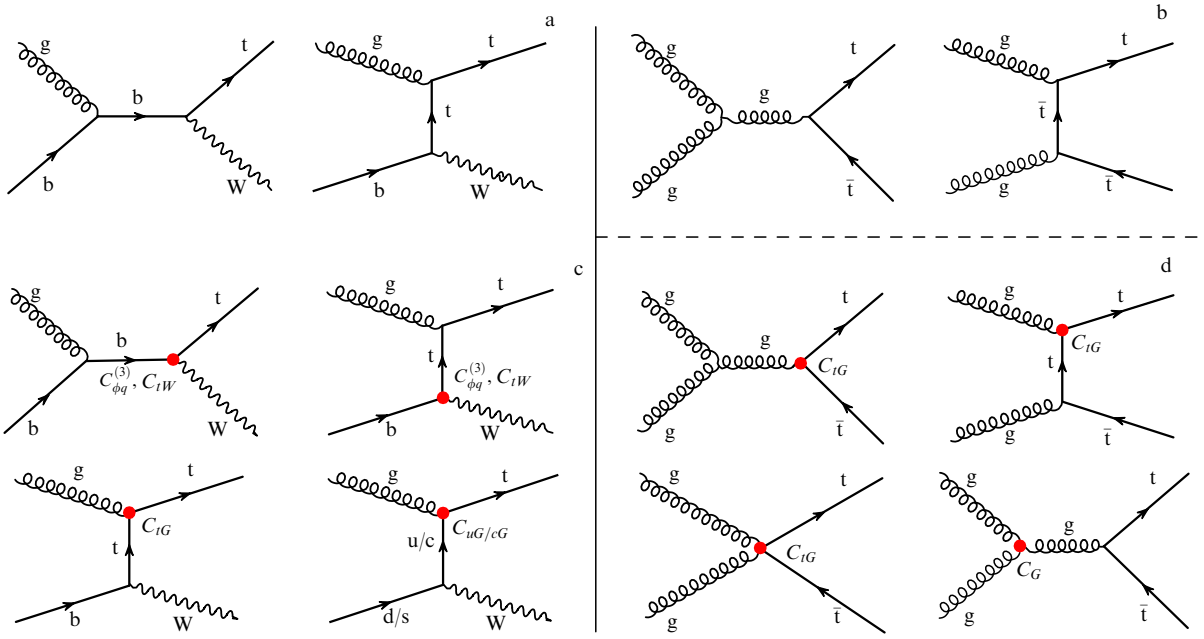

Figure 7. (a,b) Feynman diagrams that make the leading tree-level contribution to the process of single t-quark production in the mode of associative production with a W-boson gb → tW and to the process of pair t-quark production gg → tt̄. (c, d) Symbolically shown Feynman diagrams of single and pair t-quark production with selection of vertices to which SMEFT operators $O_{\phi q}^{(3)}$, O_{tW}, $O_{u(c)G}$, O_{tG}, and O_G contribute [75].

W boson. Therefore, this process allows studying the operators contributing to the above vertices and imposing bounds on the corresponding Wilson coefficients.

The CMS collaboration performed an analysis to impose direct constraints on the SMEFT operators

$$O_{tG}\,,\ O_G\,,\ O_{\phi q}^{(3)}\,,\ O_{tW}\,,\ O_{u(c)G}\,,$$

which contribute to the processes caused by pair production of t-quarks and single production of a t-quark in the tW channel [75]. The individual constraints on the Wilson coefficients obtained in the experiment, presented in Fig. 8, are numerically comparable to the previously predicted theoretical values or are somewhat better [27, 31].

7.3 SMEFT deviations in t-quark couplings to the Z boson

The CMS collaboration also obtained constraints on the Wilson coefficients of operators contributing to the process of associative production of a pair of t-quarks and a Z boson [76]. As a result, the most stringent constraints on the anomalous coupling constants ttZ were found and new constraints were imposed on the Wilson coefficients in the SMEFT approach.

Theoretical calculations of the expected SMEFT contributions to this process were carried out in [32] with the QCD NLO corrections included. In the SM, calculations of the cross section for the process pp → tt̄Z at LHC energies of 8 and 13 TeV in the leading and next-to-leading approximations are given by [32]

$$\sigma_{\rm SM}^{\rm LO} = 0.21^{+41\%\ +2.4\%}_{-27\%\ -2.5\%}\ \text{pb}\,,$$
$$\sigma_{\rm SM}^{\rm NLO} = 0.227^{+7\%\ +2.8\%}_{-11\%\ -3.2\%}\ \text{pb}\,,$$
$$\sigma_{\rm SM}^{\rm LO} = 0.76^{+38\%\ +2.1\%}_{-25\%\ -2.2\%}\ \text{pb}\,,$$
$$\sigma_{\rm SM}^{\rm NLO} = 0.88^{+8\%\ +2.0\%}_{-11\%\ -2.5\%}\ \text{pb}\,,$$

where the first error is related to the variation in the renormalization and factorization scale $\mu = \mu_{\rm R} = \mu_{\rm F}$ within

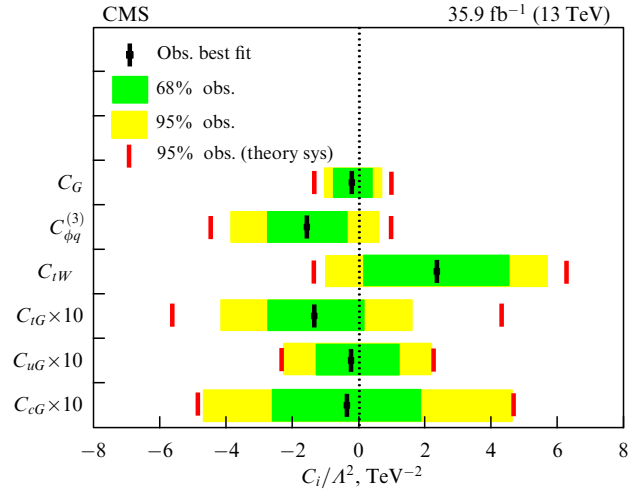

Figure 8. (Color online.) Constraints on Wilson coefficients $C_{\phi q}^{(3)}$, C_{tW}, $C_{u(c)G}$, C_{tG}, and C_G obtained in the CMS experiment at a collision energy of 13 TeV and an integrated luminosity of 35.9 fb^{-1} [75].

$m_{\rm t}/2 \leqslant \mu \leqslant 2m_{\rm t}$, and the second, to uncertainties in the MSTW2008 distribution functions chosen for the computation [77]. As can be seen from the given values, the increase in the mean of the cross sections in moving from the LO to the NLO is not so significant: the K factor is 1.09 and 1.15 for the respective energies of 8 and 13 TeV. But, when varying the μ scale, the error becomes much smaller, which indicates, as it should, a much more accurate prediction of the cross section value at the NLO level. We note that the calculation of the cross section for the process pp → tt̄Z at the NNLO level was also carried out in [78], showing a further slight improvement in accuracy, in particular, for the 13-TeV energy, the cross section is

$$\sigma_{\rm SM}^{\rm NNLO} = 0.86^{+0.07}_{-0.08}(\text{scale}) \pm 0.03(\text{PDF} + \alpha_{\rm s})\ \text{pb}\,.$$

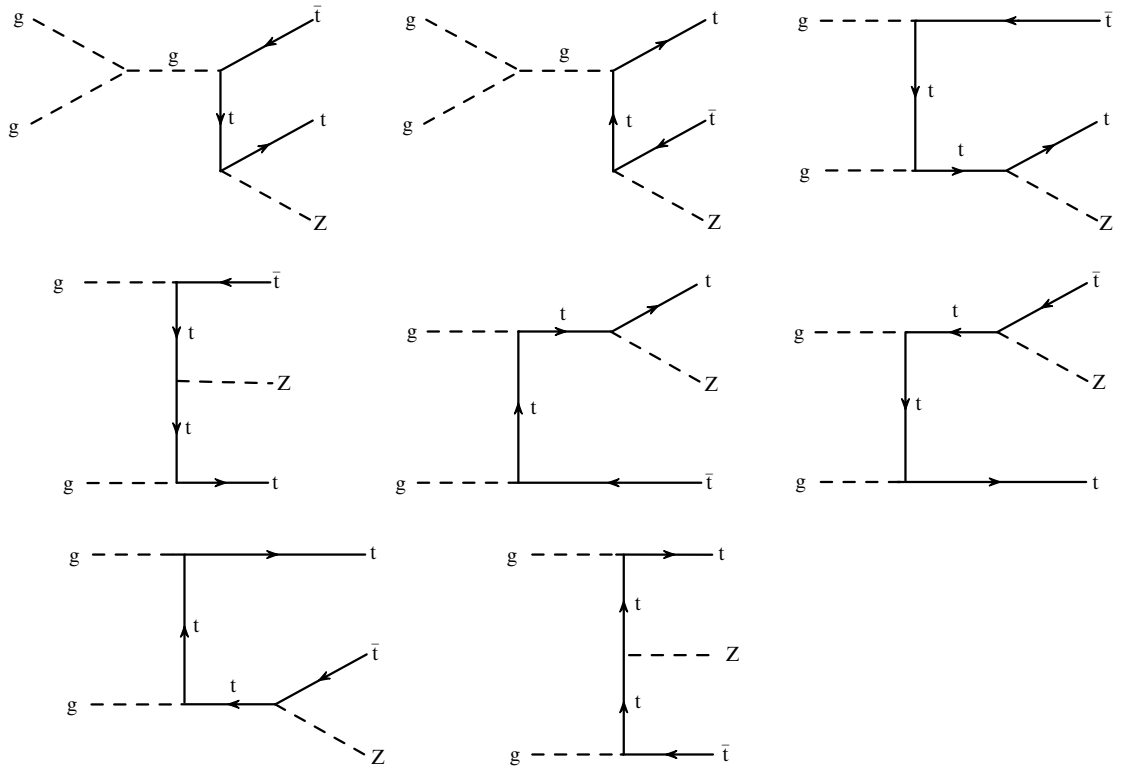

Figure 9. Feynman diagrams in the leading order for the associative production of a $t\bar{t}$ pair and a Z boson in a gluon–gluon collision.

The theoretical values obtained for the cross sections are in good agreement with the cross sections measured in the CMS [76],

$$\sigma(pp \to t\bar{t}Z) = 0.95 \pm 0.05(\text{stat.}) \pm 0.06(\text{syst.})\ \text{pb}\,,$$

and ATLAS [79],

$$\sigma(pp \to t\bar{t}Z) = 0.95 \pm 0.08(\text{stat.}) \pm 0.10(\text{syst.})\ \text{pb}\,,$$

experiments.

The complete set of Feynman diagrams that contribute in the leading order to the associative production of a $t\bar{t}$ pair and a Z boson in gluon–gluon collisions is shown in Fig. 9. It can be seen that the diagrams include the three-gluon vertex ggg and the vertices of the t-quark coupling to the gluon, $t\bar{t}g$, and to the Z boson, $t\bar{t}Z$. Additions to these vertices are given by the SMEFT operators

$$O_{tG}\,,\ O_{G}\,,\ O_{\phi q}^{(1,33)}\,,\ O_{\phi q}^{(3,33)}\,,\ O_{\phi u}^{(33)} \equiv O_{\phi t}\,,$$
$$O_{uW}^{(33)} \equiv O_{tW}\,,\ O_{uB}^{(33)} \equiv O_{tB}\,. \qquad (17)$$

As we discussed in Section 7.2, however, some of the operators are much more strongly constrained from the pair and single t-quark production processes than one would expect them to be from the $pp \to t\bar{t}Z$ process. In the analysis, therefore, only those SMEFT operators or combinations of operators are selected that have not been constrained in other analyses. The constraints on Wilson coefficients are obtained with the following combinations of operators [76]:

$$c_{tZ} = \text{Re}\left(-\sin\theta_{\text{W}} C_{uB}^{(33)} + \cos\theta_{\text{W}} C_{uW}^{(33)}\right),$$
$$c_{tZ}^{[I]} = \text{Im}\left(-\sin\theta_{\text{W}} C_{uB}^{(33)} + \cos\theta_{\text{W}} C_{uW}^{(33)}\right),$$
$$c_{\phi t} = C_{\phi u}^{(33)}\,,\quad c_{\phi Q}^{-} = C_{\phi q}^{(1,33)} - C_{\phi q}^{(3,33)}\,.$$

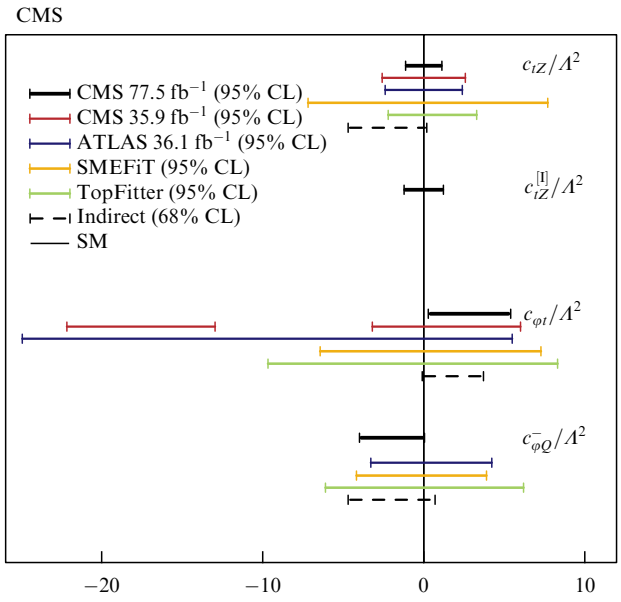

Figure 10. (Color online.) Confidence intervals at the 95% confidence level for a number of Wilson coefficients obtained by CMS [76] and ATLAS [79] collaborations compared to previous CMS results [87] and to bounds obtained from the analysis of precision electroweak measurements using SMEFiT [85] and TopFitter [61] programs, as well as to bounds given in [88] at a 68% confidence level. Vertical line corresponds to the SM, in which all Wilson coefficients vanish. The figure is taken from [76]. Scale: $\Lambda = 1$ TeV.

The resulting constraints are shown in Fig. 10. It can be seen that, at a 95% confidence level, the bounds established by the CMS [76] and ATLAS [79] collaborations are consistent both with each other and with previous CMS results [87]. The

bounds are also consistent within the accuracy with those obtained from the analysis of the results of precision electroweak measurements using the specialized software packages SMEFiT [85] and TopFitter [61]. We also note the agreement with the bounds given in [88] at a 68% confidence level. In Fig. 10, the vertical line corresponds to the SM, with all Wilson coefficients equal to zero. As can be seen, the resulting constraints are still very weak, leaving room for possible contributions from new physics.

7.4 Constraints on Wilson coefficients for SMEFT operators containing four t-quark fields

Gluon–gluon collisions make the leading contribution to the production of two t-quark–anti-t-quark pairs, $pp \to t\bar{t}t\bar{t}$, at the LHC. The cross section of this process is small: with the NLO QCD corrections taken into account, it is approximately 9.2 ± 2.4 fb [82, 83]. The addition of electroweak contributions, among which the leading ones are associated with Higgs-boson exchanges due to the large Yukawa constant of the t-quark, leads to some increase in the cross section, to about 12.0 ± 3.0 fb [84]. The cross section of this process, measured by the CMS and ATLAS collaborations with a very low accuracy so far, was approximately 13^{+11}_{-9} fb from CMS [80] and 24^{+7}_{-6} fb from ATLAS [81]. With such large errors in both experimental measurements and theoretical calculations, all experimental and theoretical results are of course consistent with each other.

In Fig. 11a–c, we show examples of three SM Feynman diagrams that contribute to the formation of two $t\bar{t}$ pairs in gluon–gluon collisions. The first two diagrams contain gluon exchanges and are related to the leading tree-level contribution in QCD. The third diagram contains an exchange by a virtual Higgs boson and is one of the leading tree-level electroweak contributions, enhanced due to the large Yukawa coupling constant of the t quark and the Higgs boson $m_t\sqrt{2}/v$. Figure 11d shows an example of one of the diagrams due to the SMEFT operators, involving four t-quark fields.

We see from Fig. 11 that the process diagrams involve the vertices $t\bar{t}g$, ggg, and $t\bar{t}h$. As in the case of the associative production of a pair of t quarks and a Z boson, the SMEFT operators contributing to these vertices are much more strongly constrained in other processes, some of which were discussed above. The $t\bar{t}t\bar{t}$ process is used to find deviations and impose bounds on the Wilson coefficients in operators contributing to the four-t-quark vertex, which is absent in the SM.

The CMS collaboration carried out the corresponding analysis and established constraints on the Wilson coefficients for four operators denoted as O^1_{tt}, O^1_{QQ}, O^1_{Qt}, and O^8_{Qt} in [80]. The relation to the notation for the Warsaw basis (2) and the notation adopted in [17] are as follows:

$O^1_{tt} \equiv O_{uu}$ for the operator class $(\bar{R}R)(\bar{R}R)$ and $O^1_{tt} \equiv O^{1(3333)}_{uu}$,

$O^1_{QQ} \equiv O^1_{qq}$ for the operator class $(\bar{L}L)(\bar{L}L)$ and $O^1_{QQ} \equiv O^{1(3333)}_{qq}$,

$O^1_{Qt} \equiv O^1_{qu}$ for the operator class $(\bar{L}L)(\bar{R}R)$ and $O^1_{Qt} \equiv O^{1(3333)}_{qu}$,

$O^8_{Qt} \equiv O^8_{qu}$ for the operator class $(\bar{L}L)(\bar{R}R)$ and $O^8_{Qt} \equiv O^{8(3333)}_{qu}$.

These operators contain products of four t-quark fields, make a contribution to the four t-quark production process $t\bar{t}t\bar{t}$, and can be explicitly expressed as

$$O^1_{tt} = \left(\bar{t}_R\gamma^\mu t_R\right)\left(\bar{t}_R\gamma^\mu t_R\right),$$

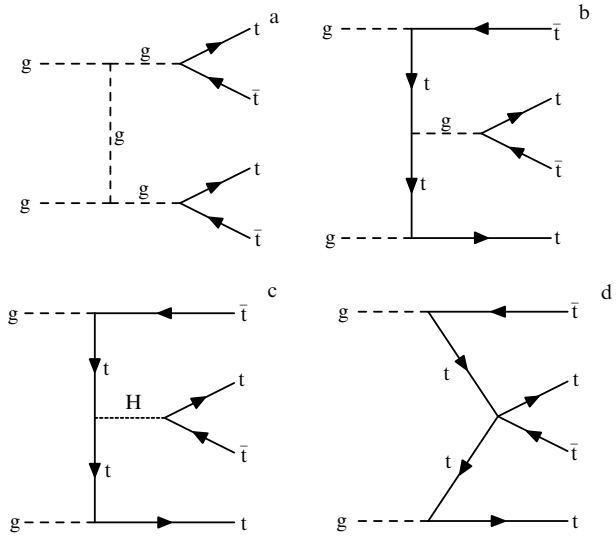

Figure 11. Examples of Feynman diagrams that contribute to the formation of two $t\bar{t}$ pairs: (a, b) QCD diagrams with a gluon exchange, (c) electroweak diagram with a Higgs boson exchange, and (d) diagram involving a vertex with four t quarks resulting from SMEFT operators.

$$O^1_{QQ} = \left(\bar{Q}_L\gamma^\mu Q_L\right)\left(\bar{Q}_L\gamma^\mu Q_L\right),$$
$$O^1_{Qt} = \left(\bar{Q}_L\gamma^\mu Q_L\right)\left(\bar{t}_R\gamma^\mu t_R\right),$$
$$O^8_{Qt} = \left(\bar{Q}_L\gamma^\mu T^A Q_L\right)\left(\bar{t}_R\gamma^\mu T^A t_R\right), \qquad (18)$$

where $Q_L \equiv q_{L3}$ denotes the weak isospin doublet of left-handed chiral fields of third-generation quarks, t_R is the right-handed chiral field of the t quark, and T^A are the generators of the SM color group $SU(3)_c$. In the analysis carried out by CMS, both linear and quadratic contributions (in $1/\Lambda^2$) of the reduced operators were taken into account. The results for the expected and observed bounds on the ratios of the coefficients to the scale squared are presented in Table 3. They are the individual bounds for coefficients, independent of the other coefficients, with only one coefficient assumed to be nonzero in the analysis and the rest considered equal to zero. In the CMS analysis in [80], it was also checked how the bounds change if nonzero values of all coefficients are allowed but the bounds of each of the $C_k/\Lambda^2 \times \text{TeV}^2$ parameters are kept in the range of -4π to 4π, formally allowed by the perturbative unitarity requirement. It was shown that the boundaries of the intervals found under this assumption are practically unchanged compared with the individual bounds listed in Table 3, given the fact that the intervals themselves are still quite wide and, hence, the accuracy of the bounds on the Wilson coefficients is low.

Table 3. Expected and observed intervals for Wilson coefficients at a 95% confidence level, obtained under the assumption that only one of the operators contributes and coefficients in the others vanish [80].

Operator	Expected C_k/Λ^2, TeV^{-2}	Observed, TeV^{-2}
O^1_{tt}	[−2.0, 1.8]	[−2.1, 2.0]
O^1_{QQ}	[−2.0, 1.8]	[−2.2, 2.0]
O^1_{Qt}	[−3.3, 3.2]	[−3.5, 3.5]
O^8_{Qt}	[−7.3, 6.1]	[−7.9, 6.6]

8. Constraints on Wilson coefficients from global data fitting

In the SMEFT approach, as discussed in Section 3, even the minimum complete set of basis operators of dimension 6, represented explicitly, for example, in the Warsaw basis form, contains 59 independent operators. Each of these gauge-invariant operators, expressed in terms of the SM fields, leads either to a modification of a number of the SM interaction vertices or to the appearance of new point-like vertices containing products of four, five, or six SM fields. As we saw in the above examples, the modification or appearance of new vertices, on the one hand, results in contributions of the same operator to different processes, and, on the other hand, means different operators contribute to the same process. When perturbative corrections are considered in terms of the SM coupling constants, it turns out that several dozen operators simultaneously contribute to many processes that are either already being studied or can be studied in experiments. For this reason, research is being actively conducted to impose bounds on the Wilson coefficients in several operators by simultaneously analyzing a large number of processes to which specific operators contribute.

This simultaneous analysis of data from different experiments, called a global fit, is carried out either with specialized computer programs such as TopFitter [61], Sfitter [86], or SMEFiT [85], or using one's own computer codes, as, for example, in [54]. The presented results of the global fit include data on precision measurements of the coupling parameters of the t quark, the Higgs boson, and the SM gauge bosons. We emphasize once again that it is extremely important to use the same basis of operators, the Warsaw basis of dimension-six operators, which makes it quite easy to compare the results of different analyses without additional complex recalculation from one basis to another, even if the chosen basis is not the most convenient or optimal in some specific cases.

As follows from formula (3), if we ignore operators of dimension 8, then both the cross section itself and any kinematical variable or observable $f_{\rm kin}^{\rm SMEFT}$ has the form of a quadratic polynomial in the Wilson coefficients C_i for dimension-six operators:

$$f_{\rm kin}^{\rm SMEFT} = f_{\rm kin}^{\rm SM} + \left(\sum_i a_i \frac{C_i^{(6)}}{\Lambda^2} + \text{h.c.}\right) + \left(\sum_{i,j} b_{ij} \frac{C_i^{(6)} C_j^{(6^*)}}{\Lambda^4} + \text{h.c.}\right), \tag{19}$$

where $f_{\rm kin}$, a_i, and b_{ij} are some functions of the momenta of the initial and final particles involved in the process under study. If unstable particles are involved in intermediate states in some of the processes, then the decay widths of these particles also depend, generally speaking, on some Wilson coefficients, and the denominators of the expressions for a_i and b_{ij} must be expanded in a series in $1/\Lambda^2$ through the order $1/\Lambda^4$. We note, however, that this circumstance is neglected in many studies. Dependences for variables or observables (19), together with experimental data, are fed into general χ^2-type functions, and minimizing the corresponding functionals allows finding (at a certain confidence level, typically 95%) the bounds for the Wilson coefficients divided by Λ^2 (C_i/Λ^2) in units of TeV^{-2}. In a number of papers, constraints are given on the dimensionless parameters $\bar{C}_i = C_i v^2/\Lambda^2$.

We briefly consider the results of the analysis in [61] in terms of the parameters $\bar{C}_i$ obtained using the TopFitter program. The analysis used data on the measurement of cross sections and some kinematical distributions for pair and single t-quark production in all available modes by the CDF (Collider Detector at Fermilab) and D0 collaborations at the Tevatron collider at the proton–antiproton collision energy $\sqrt{s} = 1.96$ TeV and the data from the ATLAS and CMS collaborations at the LHC at the proton–proton collision energies of $\sqrt{s} = 7$ and 8 TeV. The analysis included the following Warsaw-basis operators, whose relation to the original notation (1) was discussed above:

$$\begin{aligned}
&O_{qq}^{(1)} = (\bar{q}\gamma_\mu q)(\bar{q}\gamma^\mu q)\,, \quad O_{uW} = (\bar{q}\sigma^{\mu\nu}\tau^I u)\tilde{\varphi} W_{\mu\nu}^I\,,\\
&O_{\varphi q}^{(3)} = \mathrm{i}(\varphi^\dagger \overleftrightarrow{D}_\mu^I \varphi)(\bar{q}\gamma^\mu \tau^I q)\,, \quad O_{qq}^{(3)} = (\bar{q}\gamma_\mu \tau^I q)(\bar{q}\gamma^\mu \tau^I q)\,,\\
&O_{uG} = (\bar{q}\sigma^{\mu\nu} T^A u)\tilde{\varphi} G_{\mu\nu}^A\,, \quad O_{\varphi q}^{(1)} = \mathrm{i}(\varphi^\dagger \overleftrightarrow{D}_\mu \varphi)(\bar{q}\gamma^\mu q)\,,\\
&O_{uu} = (\bar{u}\gamma_\mu u)(\bar{u}\gamma^\mu u)\,, \quad O_G = f_{ABC} G_\mu^{A\nu} G_\nu^{B\lambda} G_\lambda^{C\mu}\,,\\
&O_{uB} = (\bar{q}\sigma^{\mu\nu} u)\tilde{\varphi} B_{\mu\nu}\,, \quad O_{qu}^{(8)} = (\bar{q}\gamma_\mu T^A q)(\bar{u}\gamma^\mu T^A u)\,,\\
&O_{\tilde{G}} = f_{ABC} \tilde{G}_\mu^{A\nu} G_\nu^{B\lambda} G_\lambda^{C\mu}\,, \quad O_{\varphi u} = (\varphi^\dagger \mathrm{i} \overleftrightarrow{D}_\mu \varphi)(\bar{u}\gamma^\mu u)\,,\\
&O_{qd}^{(8)} = (\bar{q}\gamma_\mu T^A q)(\bar{d}\gamma^\mu T^A d)\,, \quad O_{\varphi G} = (\varphi^\dagger \varphi) G_{\mu\nu}^A G^{A\mu\nu}\,,\\
&O_{\varphi\tilde{G}} = (\varphi^\dagger \varphi)\tilde{G}_{\mu\nu}^A G^{A\mu\nu}\,, \quad O_{ud}^{(8)} = (\bar{u}\gamma_\mu T^A u)(\bar{d}\gamma^\mu T^A d)\,.
\end{aligned} \tag{20}$$

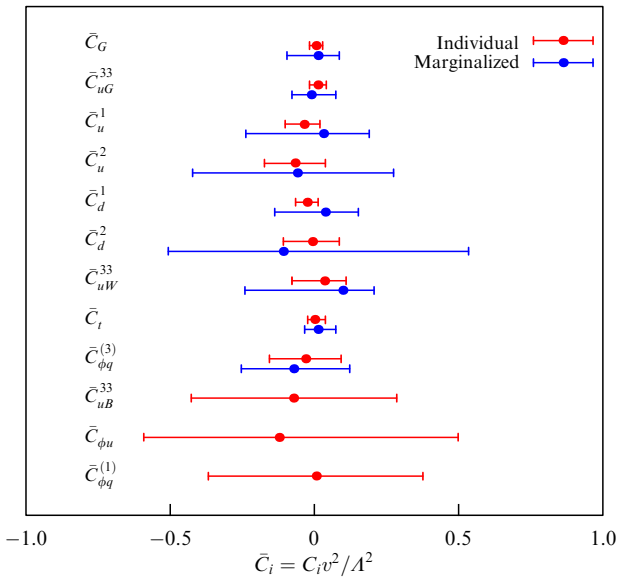

Figure 12. (Color online.) Bounds at a 95% confidence level for coefficients in dimension-six operators contributing to pair and single t-quark production, in the case of individual limits, with only one operator contributing and the coefficients for others assumed to be equal to zero (red), and in the case where all coefficients can be different from zero (blue). Results were obtained in [61].

Figure 12 shows the bounds [61] for the coefficients $\bar{C}_i$ for dimension-six operators (20), which contribute to pair and single t-quark production. Bounds at the 95% confidence level are given in two cases: that of individual bounds, when only one operator contributes and the coefficients for the others are assumed to be zero (indicated by red horizontal lines), and the case of so-called marginalized bounds, with the contributions of all operators taken into account simultaneously, i.e., when all relevant coefficients can be nonzero (indicated by blue horizontal lines). Figure 12 shows that, as it should be, individual bounds are much more stringent than marginalized ones. Constraints on the last three coefficients in the operators $O_{uB}^{(33)}$, $O_{\phi u} \equiv O_{\phi u}^{(33)}$, and $O_{\phi q}^1 \equiv O_{\phi q}^{(1,33)}$, which

contribute to the process of associative pair production of t quarks and the Z boson, Eqn (17), are so weak that only the individual bounds are shown in Fig. 12.

Data from the second LHC run (RUN2) at the collision energy $\sqrt{s} = 13$ TeV were also added and taken into account in [89]. The corresponding analysis was carried out using the Sfitter software package [90, 91], which had been developed for studying supersymmetry and the Higgs sector, but was used for global analysis and imposing constraints on the Wilson coefficients in the SMEFT approach [86, 89]. In the analysis in [89], the following notation for quark fields was used:

$$q_i = (u_{\mathrm{L}}^i, d_{\mathrm{L}}^i)\,, \quad u_i = u_{\mathrm{R}}^i\,, \quad d_i = d_{\mathrm{R}}^i\,, \quad i = 1,2\,, \qquad Q = (t_{\mathrm{L}}, b_{\mathrm{L}})\,, \quad t = t_{\mathrm{R}}\,, \quad b = b_{\mathrm{R}}\,. \tag{21}$$

The operators containing quark and boson fields are related by simple redefinitions to the Warsaw-basis fields (see Section 7 for details):

$$O_{\phi Q}^1 \equiv (\phi^\dagger\, i\overleftrightarrow{D_\mu}\,\phi)(\bar{Q}\gamma^\mu Q) = \mathcal{O}_{\phi q}^{1(33)}\,,$$
$$^\ddagger O_{tB} \equiv (\bar{Q}\sigma^{\mu\nu} t)\,\tilde{\phi}\, B_{\mu\nu} = {}^\ddagger\mathcal{O}_{uB}^{(33)}\,,$$
$$O_{\phi Q}^3 \equiv (\phi^\dagger\, i\overleftrightarrow{D_\mu^I}\,\phi)(\bar{Q}\gamma^\mu \tau^I Q) = \mathcal{O}_{\phi q}^{3(33)}\,,$$
$$^\ddagger O_{tW} \equiv (\bar{Q}\sigma^{\mu\nu} t)\,\tau^I\tilde{\phi}\, W_{\mu\nu}^I = {}^\ddagger\mathcal{O}_{uW}^{(33)}\,,$$
$$O_{\phi t} \equiv (\phi^\dagger\, i\overleftrightarrow{D_\mu}\phi)(\bar{t}\gamma^\mu t) = \mathcal{O}_{\phi u}^{(33)}\,,$$
$$^\ddagger O_{bW} \equiv (\bar{Q}\sigma^{\mu\nu} b)\,\tau^I\phi\, W_{\mu\nu}^I = {}^\ddagger\mathcal{O}_{dW}^{(33)}\,,$$
$$^\ddagger O_{\phi tb} \equiv (\tilde{\phi}^\dagger i D_\mu \phi)(\bar{t}\gamma^\mu b) = {}^\ddagger\mathcal{O}_{\phi ud}^{(33)}\,,$$
$$^\ddagger O_{tG} \equiv (\bar{Q}\sigma^{\mu\nu} T^A t)\,\tilde{\phi}\, G_{\mu\nu}^A = {}^\ddagger\mathcal{O}_{uG}^{(33)}\,.$$

The four-quark operators are in some cases expressed in terms of linear combinations of Warsaw-basis operators using Fierz-type identities:

$$O_{Qq}^{1,8} \equiv (\bar{Q}\gamma_\mu T^A Q)(\bar{q}_i\gamma^\mu T^A q_i) = -\frac{1}{6}\,\mathcal{O}_{qq}^{1(33ii)} + \frac{1}{4}\,\mathcal{O}_{qq}^{1(3ii3)} + \frac{1}{4}\,\mathcal{O}_{qq}^{3(3ii3)}\,,$$
$$O_{Qq}^{3,8} \equiv (\bar{Q}\gamma_\mu T^A \tau^I Q)(\bar{q}_i\gamma^\mu T^A \tau^I q_i) = -\frac{1}{6}\,\mathcal{O}_{qq}^{3(33ii)} + \frac{3}{4}\,\mathcal{O}_{qq}^{1(3ii3)} - \frac{1}{4}\,\mathcal{O}_{qq}^{3(3ii3)}\,,$$
$$O_{Qq}^{1,1} \equiv (\bar{Q}\gamma_\mu Q)(\bar{q}_i\gamma^\mu q_i) = \mathcal{O}_{qq}^{1(33ii)}\,,$$
$$O_{Qq}^{3,1} \equiv (\bar{Q}\gamma_\mu \tau^I Q)(\bar{q}_i\gamma^\mu \tau^I q_i) = \mathcal{O}_{qq}^{3(33ii)}\,,$$
$$O_{tu}^8 \equiv (\bar{t}\gamma_\mu T^A t)(\bar{u}_i\gamma^\mu T^A u_i) = -\frac{1}{6}\,\mathcal{O}_{uu}^{(33ii)} + \frac{1}{2}\,\mathcal{O}_{uu}^{(3ii3)}\,,$$
$$O_{tu}^1 \equiv (\bar{t}\gamma_\mu t)(\bar{u}_i\gamma^\mu u_i) = \mathcal{O}_{uu}^{(33ii)}\,,$$
$$O_{td}^8 \equiv (\bar{t}\gamma^\mu T^A t)(\bar{d}_i\gamma_\mu T^A d_i) = \mathcal{O}_{ud}^{8(33ii)}\,,$$
$$O_{td}^1 \equiv (\bar{t}\gamma^\mu t)(\bar{d}_i\gamma_\mu d_i) = \mathcal{O}_{ud}^{1(33ii)}\,,$$
$$O_{Qu}^8 \equiv (\bar{Q}\gamma^\mu T^A Q)(\bar{u}_i\gamma_\mu T^A u_i) = \mathcal{O}_{qu}^{8(33ii)}\,,$$
$$O_{Qu}^1 \equiv (\bar{Q}\gamma^\mu Q)(\bar{u}_i\gamma_\mu u_i) = \mathcal{O}_{qu}^{1(33ii)}\,,$$
$$O_{Qd}^8 \equiv (\bar{Q}\gamma^\mu T^A Q)(\bar{d}_i\gamma_\mu T^A d_i) = \mathcal{O}_{qd}^{8(33ii)}\,,$$
$$O_{Qd}^1 \equiv (\bar{Q}\gamma^\mu Q)(\bar{d}_i\gamma_\mu d_i) = \mathcal{O}_{qd}^{1(33ii)}\,,$$
$$O_{tq}^8 \equiv (\bar{q}_i\gamma^\mu T^A q_i)(\bar{t}\gamma_\mu T^A t) = \mathcal{O}_{qu}^{8(ii33)}\,,$$
$$O_{tq}^1 \equiv (\bar{q}_i\gamma^\mu q_i)(\bar{t}\gamma_\mu t) = \mathcal{O}_{qu}^{1(ii33)}\,.$$

These relations are convenient in the analysis of certain specific processes, but making direct comparisons with other results is somewhat difficult. We once again give the exact formulas for the Higgs field in the unitary gauge, $\phi = (0, (1/\sqrt{2})(v+h))^\top$, $\tilde{\phi} = i\sigma_2\,\phi^*$, and for covariant derivatives, $D_\mu = \partial_\mu - \mathrm{i}g_2 W_\mu^I \tau^I/2 - \mathrm{i}g_1 B_\mu Y$, where τ^I are the Pauli matrices in accordance with the notation of the Warsaw basis. We recall that, in the original notation of the Warsaw basis, the Higgs field doublet ϕ is denoted as H.

The results for the bounds imposed on the Wilson coefficients are shown in Fig. 13 [89]. For each coefficient, bounds are given for two confidence levels: 95% (larger intervals) and 68% (smaller intervals). The blue, green, and red colors indicate bounds based on fitting data on measurements of the characteristics of pair t-quark production, single t-quark production, and a joint fit of these two types of data. As expected, the joint bounds from the entire data set are somewhat more stringent. To compare the results in [61] and [89], the bounds shown in Fig. 12 must be multiplied by the factor $(1\ \mathrm{TeV}/v_{\mathrm{SM}})^2$, where $v_{\mathrm{SM}} = 246$ GeV is the vacuum expectation value of the SM Higgs field.

The next step in the study of global constraints on the Wilson coefficients was made in [85] using the SMEFiT computer environment. In that study, the authors included only those Warsaw basis operators that appear in processes with pair ($t\bar{t} + X$), single ($t + X$ and $\bar{t} + X$), pair associative ($t\bar{t}W + X$, $t\bar{t}Z + X$, and $t\bar{t}h + X$), and single associative ($tZ + X$ and $\bar{t}Z + X$) production of the t-quark and electroweak bosons.

We note that the SMEFiT computer environment can also be used for a wider range of processes, involving not only the t quark. A feature of the study compared to the previous ones was that the analysis included all the existing results on the NLO QCD corrections to the contributions of SMEFT operators, an analysis was made of how significant the contributions to the characteristics of processes of the order of $1/\Lambda^4$ are, and cutoffs were introduced into the calculations of the contributions so as to not go beyond the SMEFT (see the discussion of these aspects in the preceding sections). For pair and single production processes, the NLO QCD corrections to the total cross sections and distributions were taken

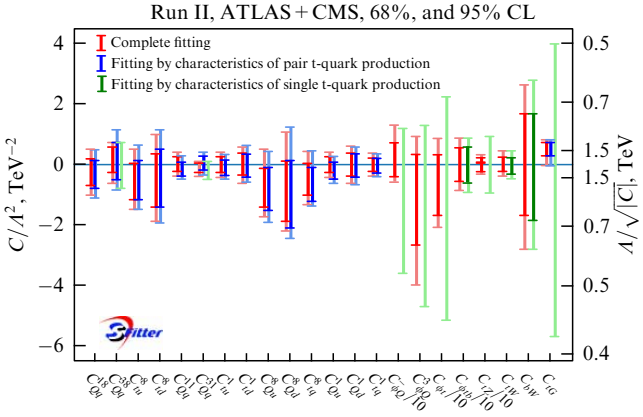

Figure 13. (Color online.) Bounds on the Wilson coefficients at 95% (larger intervals) and 68% (smaller intervals) confidence levels based on global data fitting from measurements of t-quark pair production characteristics (blue), single t-quark production (green), and complete fitting of all data on t-quark production (red). Analysis was carried out in [89].

Table 4. Notation in [85] for different types of operators, for fitting variables (degrees of freedom) c_j, and for their expressions in terms of Wilson coefficients of the Warsaw basis.*

Operator type	Notation	Fitting parameters	Wilson coefficients in operators
$QQQQ$	OQQ1	c_{QQ}^{1}	$2C_{qq}^{1(3333)} - \frac{2}{3}C_{qq}^{3(3333)}$
	OQQ8	c_{QQ}^{8}	$8C_{qq}^{3(3333)}$
	OQt1	c_{Qt}^{1}	$C_{qu}^{1(3333)}$
	OQt8	c_{Qt}^{8}	$C_{qu}^{8(3333)}$
	OQb1	c_{Qb}^{1}	$C_{qd}^{1(3333)}$
	OQb8	c_{Qb}^{8}	$C_{qd}^{8(3333)}$
	Ott1	c_{tt}^{1}	$C_{uu}^{(3333)}$
	Otb1	c_{tb}^{1}	$C_{ud}^{1(3333)}$
	Otb8	c_{tb}^{8}	$C_{ud}^{8(3333)}$
	OQtQb1	c_{QtQb}^{1}	$C_{quqd}^{1(3333)}$
	OQtQb8	c_{QtQb}^{8}	$C_{quqd}^{8(3333)}$
$QQqq$	O81qq	$c_{Qq}^{1,8}$	$C_{qq}^{1(i33i)} + 3C_{qq}^{3(i33i)}$
	O11qq	$c_{Qq}^{1,1}$	$C_{qq}^{1(ii33)} + \frac{1}{6}C_{qq}^{1(i33i)} + \frac{1}{2}C_{qq}^{3(i33i)}$
	O83qq	$c_{Qq}^{3,8}$	$C_{qq}^{1(i33i)} - C_{qq}^{3(i33i)}$
	O13qq	$c_{Qq}^{3,1}$	$C_{qq}^{3(ii33)} + \frac{1}{6}(C_{qq}^{1(i33i)} - C_{qq}^{3(i33i)})$
	O8qt	c_{tq}^{8}	$C_{qu}^{8(ii33)}$
	O1qt	c_{tq}^{1}	$C_{qu}^{1(ii33)}$
	O8ut	c_{tu}^{8}	$2C_{uu}^{(i33i)}$
	O1ut	c_{tu}^{1}	$C_{uu}^{(ii33)} + \frac{1}{3}C_{uu}^{(i33i)}$
	O8qu	c_{Qu}^{8}	$C_{qu}^{8(33ii)}$
	O1qu	c_{Qu}^{1}	$C_{qu}^{1(33ii)}$
	O8dt	c_{td}^{8}	$C_{ud}^{8(33ii)}$
	O1dt	c_{td}^{1}	$C_{ud}^{1(33ii)}$
	O8qd	c_{Qd}^{8}	$C_{qd}^{8(33ii)}$
	O1qd	c_{Qd}^{1}	$C_{qd}^{1(33ii)}$
$QQ + V, G, \varphi$	OtG	c_{tG}	$\mathrm{Re}\{C_{uG}^{(33)}\}$
	OtW	c_{tW}	$\mathrm{Re}\{C_{uW}^{(33)}\}$
	ObW	c_{bW}	$\mathrm{Re}\{C_{dW}^{(33)}\}$
	OtZ	c_{tZ}	$\mathrm{Re}\{-s_W C_{uB}^{(33)} + c_W C_{uW}^{(33)}\}$
	Off	$c_{\varphi tb}$	$\mathrm{Re}\{C_{\varphi ud}^{(33)}\}$
	Ofq3	$c_{\varphi Q}^{3}$	$C_{\varphi q}^{3(33)}$
	OpQM	$c_{\varphi Q}^{-}$	$C_{\varphi q}^{1(33)} - C_{\varphi q}^{3(33)}$
	Opt	$c_{\varphi t}$	$C_{\varphi u}^{(33)}$
	Otp	$c_{t\varphi}$	$\mathrm{Re}\{C_{u\varphi}^{(33)}\}$

* Operators are divided into three classes: four-quark ($QQQQ$) with fields of third-generation heavy quarks, four-quark with two heavy and two light quark fields ($QQqq$), and operators coupling the fields of two heavy quarks to gauge boson fields or the Higgs boson field ($QQ + V$, G, φ).

into account, and in the case of associative production with electroweak bosons, the cross sections for processes in the LO were multiplied by K-factors. In the SMEFiT code, the notation for the SMEFT operators from [17] was used, with explicitly written indices for generations: $i = 3$ corresponds to fermions of the third generation, and $i = 1, 2$, to fermions of the first two generations. The explicit form of the Wilson coefficients of the operators (the notation for the C coefficients being exactly the same as for the corresponding O operators) is given in Table 4 [85]. As in the analysis in [89],

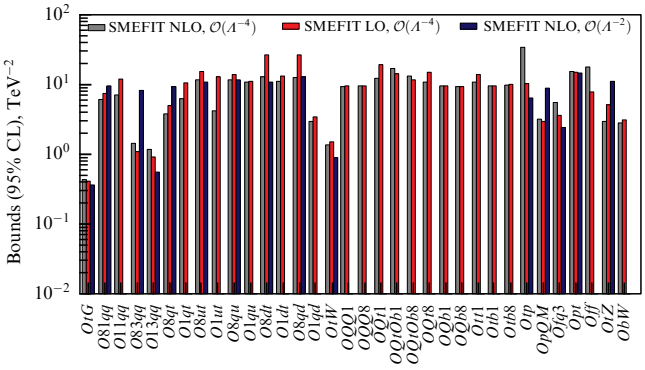

Figure 14. (Color online.) Results of the global fitting of data on the measurement of the characteristics of processes involving the t quark, to which certain SMEFT operators of dimension 6 contribute, including only the LO QCD contributions and only in the linear approximation $\mathcal{O}(\Lambda^{-2})$ (black bars), including only the LO QCD contributions together with contributions of the order of $\mathcal{O}(\Lambda^{-4})$ (red bars), and including the LO QCD contributions together with the NLO corrections and order-$\mathcal{O}(\Lambda^{-4})$ contributions (gray bars). Results were presented by the SMEFiT group [85].

linear combinations of the Warsaw basis operators are sometimes used in [85] for fitting when these linear combinations contribute to certain processes and the combinations orthogonal to them form 'flat' directions in the parameter space to which the experiment is currently insensitive. As an example of the results obtained in [85], we present a figure from that paper: Fig. 14 shows the bounds at a 95% confidence level for the coefficients in the operators in the notation given in Table 4, obtained from the global fitting of data on measuring the characteristics of processes involving the t quark. Three variants of analysis are compared. The black bars show the bounds in the case where only the leading contributions in the coupling constant of strong interactions (LO QCD) were taken into account and only in the linear approximation in Λ^{-2}. The red bars show the bounds obtained when only the LO QCD contributions were taken into account, together with order-Λ^{-4} contributions to the cross sections and distributions from quadratic combinations of operators. Finally, the gray bars show the bounds when both the NLO QCD corrections and contributions of the order of Λ^{-4} are taken into account.

Interestingly, for some operators containing four heavy-quarks fields, there are no black bars, which gives just an example of the situation discussed above, when interference with the SM alone, providing contributions of the order of Λ^{-2}, turns out to be insufficient to impose any constraints. It is worth noting that in most cases the constraints on the coefficients in the operators become more stringent if QCD NLO perturbative corrections, order-Λ^{-4} contributions, or both are taken into account in the calculations and analysis.

Global fitting was carried out not only for operators contributing to processes involving the t quark but also for operators contributing to various processes involving electroweak gauge bosons. In the analysis presented in [54], the fit simultaneously includes so-called precision electroweak data at the LEP1 (Large Electron–Positron collider 1) at the Z-boson pole, measurements of the W-boson masses using the Tevatron and LHC colliders, measurements of various characteristics of the processes $e^+e^- \to W^+W^- \to 4$ fermions at the LEP2 collider, pair production of W^+W^- bosons at the LHC, and data on Higgs boson production at the LHC in both RUN1 and RUN2. The following 20 Warsaw basis SMEFT operators were included in the analysis:

$$\begin{aligned}
\mathcal{L}_{\text{SMEFT}}^{\text{Warsaw}} \supset\ & \frac{\bar{C}_{Hl}^{(3)}}{v^2}(H^\dagger i\overleftrightarrow{D}_\mu^I H)(\bar{l}\tau^I\gamma^\mu l) + \frac{\bar{C}_{Hl}^{(1)}}{v^2}(H^\dagger i\overleftrightarrow{D}_\mu H)(\bar{l}\gamma^\mu l) \\
& + \frac{\bar{C}_{ll}}{v^2}(\bar{l}\gamma_\mu l)(\bar{l}\gamma^\mu l) + \frac{\bar{C}_{HD}}{v^2}\left|H^\dagger D_\mu H\right|^2 \\
& + \frac{\bar{C}_{HWB}}{v^2}\, H^\dagger\tau^I H\, W_{\mu\nu}^I B^{\mu\nu} + \frac{\bar{C}_{He}}{v^2}(H^\dagger i\overleftrightarrow{D}_\mu H)(\bar{e}\gamma^\mu e) \\
& + \frac{\bar{C}_{Hu}}{v^2}(H^\dagger i\overleftrightarrow{D}_\mu H)(\bar{u}\gamma^\mu u) + \frac{\bar{C}_{Hd}}{v^2}(H^\dagger i\overleftrightarrow{D}_\mu H)(\bar{d}\gamma^\mu d) \\
& + \frac{\bar{C}_{Hq}^{(3)}}{v^2}(H^\dagger i\overleftrightarrow{D}_\mu^I H)(\bar{q}\tau^I\gamma^\mu q) + \frac{\bar{C}_{Hq}^{(1)}}{v^2}(H^\dagger i\overleftrightarrow{D}_\mu H)(\bar{q}\gamma^\mu q) \\
& + \frac{\bar{C}_W}{v^2}\,\epsilon^{IJK} W_\mu^{I\nu} W_\nu^{J\rho} W_\rho^{K\mu}\,, \qquad (22)
\end{aligned}$$

$$\begin{aligned}
\mathcal{L}_{\text{SMEFT}}^{\text{Warsaw}} \supset\ & \frac{\bar{C}_{eH}}{v^2} y_e (H^\dagger H)(\bar{l}eH) + \frac{\bar{C}_{dH}}{v^2}\, y_d (H^\dagger H)(\bar{q}dH) \\
& + \frac{\bar{C}_{uH}}{v^2}\, y_u (H^\dagger H)(\bar{q}u\tilde{H}) + \frac{\bar{C}_G}{v^2} f^{ABC} G_\mu^{A\nu} G_\nu^{B\rho} G_\rho^{C\mu} \\
& + \frac{\bar{C}_{H\Box}}{v^2}(H^\dagger H)\Box(H^\dagger H) + \frac{\bar{C}_{uG}}{v^2}\, y_u(\bar{q}\sigma^{\mu\nu}T^A u)\tilde{H} G_{\mu\nu}^A \\
& + \frac{\bar{C}_{HW}}{v^2} H^\dagger H\, W_{\mu\nu}^I W^{I\mu\nu} + \frac{\bar{C}_{HB}}{v^2}\, H^\dagger H\, B_{\mu\nu} B^{\mu\nu} \\
& + \frac{\bar{C}_{HG}}{v^2}\, H^\dagger H\, G_{\mu\nu}^A G^{A\mu\nu}\,, \qquad (23)
\end{aligned}$$

where the notation $\bar{C}$ relates to the Wilson coefficients in the Warsaw basis operators as

$$\bar{C} \equiv \frac{v^2}{\Lambda^2}\, C\,. \qquad (24)$$

In (22), there are 11 operators that modify either the self-coupling of gauge bosons or the coupling of fermions to gauge bosons, and 9 other operators (23) contribute to changes in the couplings associated with the Higgs boson.

The Higgs field doublet is denoted by H in [54], just as in the original work of the Warsaw group [14]. Figure 15 shows the constraints on the Wilson coefficients for the Warsaw basis operators defined in (22) and (23). At a 95% confidence level, constraints are given in the case where all operators are included in the analysis (marginalized case, Fig. 15a), and in the case where operators are included in the analysis individually (individual case, Fig. 15b). The blue color shows the wider bounds for the analysis including all the data except those obtained in the second run of the LHC, and the orange color shows more stringent bounds obtained when taking all the data into account. We see from a comparison of constraints in Figs 15a and b that the individual bounds are again much more stringent than in the case where all operators are included in the analysis (we note the different ranges of values for the vertical axis bounds in Figs 15a and b). This is fully consistent with expectations and the discussed results of other studies. We emphasize that none of the cited studies on global data fitting show any significant deviations from the SM predictions, thus again demonstrating the reliability of the SM predictions.

9. SMEFT and its relation to specific models

The SMEFT formalism allows consistently parameterizing deviations from the SM predictions in a gauge-invariant

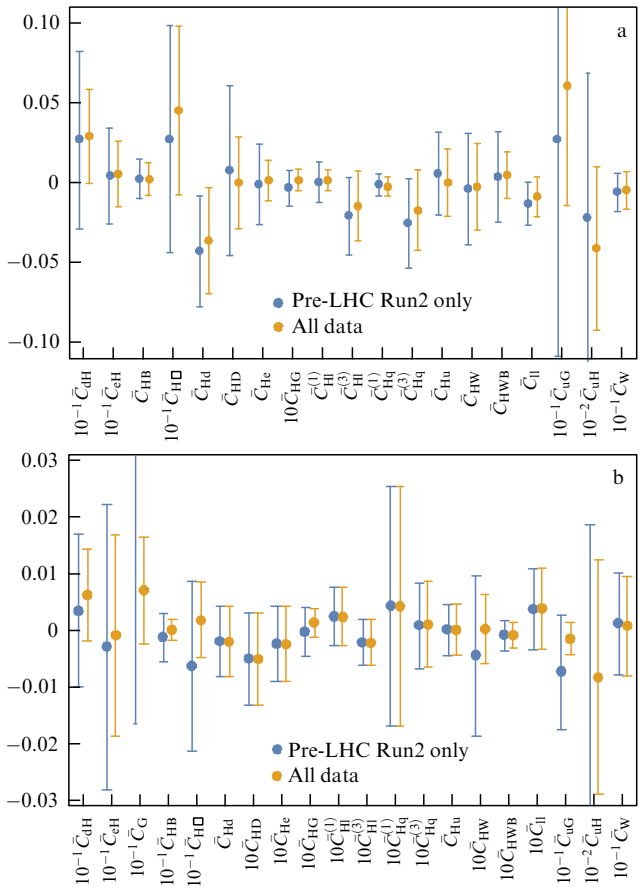

Figure 15. (Color online.) Bounds on the Wilson coefficients for the Warsaw basis operators at a 95% confidence level in cases where (a) all operators are included in the analysis, and (b) the operators are included in the analysis individually, one at a time. Blue color shows bounds obtained by including all data except that of the second LHC run (pre-LHC Run2 only); orange color shows bounds obtained when taking all data into account. Results were presented in [54].

manner, comparing constraints obtained in different experiments, and comparing these constraints with different theoretical predictions. So far, no significant deviations have been found, and hence the validity of the SM is confirmed with increasing accuracy.

However, we can imagine that some deviations are statistically reliably discovered. Then, there is the serious problem of interpreting the obtained deviations. From this standpoint, it is interesting to study which operators of dimension 6 appear as predictions in certain models or scenarios beyond the SM (BSM) [92–95]. A dedicated program code, CoDEx [96], was developed to obtain the type of operators and their coefficients arising when integrating out heavy degrees of freedom in various models beyond the SM, and to compare with the SMEFT Wilson coefficients in the Warsaw basis. An important element in the analysis is the matching procedure. The BSM operator coefficient is given on some scale of the new physics, e.g., of the order of several TeV, and a comparison with the data, strictly speaking, is made on the electroweak scale. Therefore, as discussed above, it is necessary to take into account the change in the coefficients with a change in scale in accordance with the renormalization group predictions, which is explicitly represented in the following formula in the notation adopted in [92]:

$$C_i(M_Z) = C_i(\Lambda) - \frac{1}{16\pi^2}\,\dot{C}_i \log\left(\frac{\Lambda}{M_Z}\right), \quad \dot{C}_i \equiv \gamma_{ij} C_j, \quad (25)$$

where γ_{ij} is the matrix of anomalous dimensions, all of whose entries are listed in [15, 21, 22].

As an illustration, we consider a sufficiently simple example [92] where a real scalar field representing a singlet with respect to the SM gauge group is added. The interaction potential can then be written as

$$V = -\mu_h^2|H|^2 + \frac{\lambda_h}{2}\left(|H|^2\right)^2 + \frac{m_S^2}{2}\,\tilde{S}^2 + A|H|^2\tilde{S} + \frac{\kappa}{2}\,|H|^2\tilde{S}^2 + \frac{m}{6}\,\tilde{S}^3 + \frac{\lambda_S}{24}\,\tilde{S}^4\,. \quad (26)$$

The parameters in potential (26) can be redefined such that the vacuum expectation value of the scalar field vanishes, $\langle\tilde{S}\rangle = 0$. After spontaneous symmetry breaking, two fields in the unitary gauge, $\tilde{h}$ from the doublet $H_0 = (\tilde{h} + v)/\sqrt{2}$ and $\tilde{S}$, mix into two physical fields h and S,

$$\begin{aligned} h &= \cos\theta\,\tilde{h} - \sin\theta\,\tilde{S}\,, \\ S &= \sin\theta\,\tilde{h} + \cos\theta\,\tilde{S}\,, \end{aligned} \quad (27)$$

with physical masses M_H and M. In the case $M \gg M_H$, the heavy scalar field S can be integrated out, which then gives dimension-six operators of the Warsaw basis. In this case, two operators arise,

$$O_H = (H^\dagger H)^3\,, \quad O_{H\Box} = (H^\dagger H)\Box(H^\dagger H)\,,$$

with the Wilson coefficients that in the large-M limit have the form [92]

$$\begin{aligned} \frac{C_{H\Box}}{\Lambda^2} &= -\frac{1}{2v^2}\tan^2\theta\,, \\ C_H &= -C_{H\Box}\left(\frac{m}{3v}\tan\theta - \kappa\right). \end{aligned} \quad (28)$$

In the general case, the analysis and presentation of the results are rather complicated [92]. In a simpler case, where the Z_2 symmetry condition is initially imposed on potential (26), the operator $O_H = (H^\dagger H)^3$ does not arise, which corresponds to $C_H = 0$. Then, in fact, the only parameter through which the coefficient $C_{H\Box}$ is expressed is the mixing angle θ. Given the logarithmic renormalization-group dependence of the Wilson coefficient $C_{H\Box}$ on the matching scale Λ, which is chosen to be 1 TeV, the upper bound θ is obtained from fitting the data measured on the electroweak scale. The result of such fitting is shown in Fig. 16, which shows the upper bound for the Wilson coefficient $C_{H\Box}$ at a 95% confidence level, expressed in terms of the scalar field mixing angle $\sin\theta$. Using the renormalization-group evolution of this Wilson coefficient in the range from the matching scale $\Lambda = 1$ TeV to the electroweak scale gives the bound on $\sin\theta$ shown in the figure. The results are presented for several analyses. The dark dashed curve shows the bound when only electroweak precision observation (EWPO) data were taken into account; the solid blue curve corresponds to the bound when only measurements related to the Higgs boson and pair production of electroweak bosons (Higgs + Diboson) are taken into

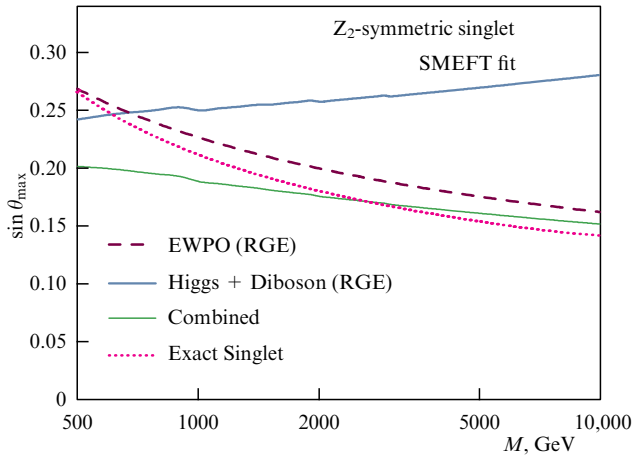

Figure 16. Upper bound at a 95% confidence level for the SMEFT $C_{H\Box}$ Wilson coefficient expressed in terms of the mixing angle $\sin\theta$, taking into account the renormalization group evolution (RGE) of this Wilson coefficient from the matching scale $\Lambda = 1$ TeV to the electroweak scale. Results were presented in [92].

account; the solid green line shows the bound taking all the data into account (Combined); the dashed purple line, shown for comparison, corresponds to the general mixing angle constraint without the Z_2 symmetry assumption (Exact singlet).

The operators from the full set of SMEFT operators predicted in a particular model and the predicted constraints on the corresponding Wilson coefficients for these operators are hallmarks of the model. In [92], a comparative analysis of the operators that arise upon integrating out heavy particles was carried out, not only for the model with an additional scalar but also for the two-Higgs doublet model (2HDM) and the vector-like fermion model (VLF), with a fermion whose left and right chiral modes are coupled to gauge bosons in the same way, etc. If some significant deviations from zero in the Wilson coefficients are found experimentally, they can be compared with the predicted bounds for different models, and thus information can be obtained as to which of the models is more likely to be the next step beyond the SM.

10. Conclusion

We have briefly discussed the SMEFT formalism, its evident advantages, and emerging problems.

We note that, after the discovery of the Higgs boson, one of the main tasks, or maybe the main task of the LHC and the discussed future colliders, is to search for new effects beyond those predicted by the Standard Model. However, intensive searches for manifestations of new physics, including the effects expected in various extensions of the SM, have not yet yielded any significant results. Accordingly, the bounds on the masses of possible new particles and states are shifted in some cases to the range of several TeV, as can be seen from Figs 1 and 2. Of course, it must be kept in mind that many bounds are model-dependent; in particular, certain scenarios are usually assumed for the characteristic coupling constants of new particles to SM particles. Smaller coupling constants would lead to a shift in the mass bounds toward lower values. Therefore, it cannot be ruled out that in such cases an increase in the collider luminosity can lead to the discovery of new particles with lower masses and smaller coupling constants.

Nevertheless, due to the negative results of direct searches for new particles and in the absence of detection of any new effects predicted in various models beyond the SM framework, attention is focused on predicting, modeling, and searching for possible small deviations from the SM in the features of the processes under study, such as cross sections, kinematical distributions, and decay widths and branching ratios. The SMEFT formalism is a well-motivated and valid field-theory approach to the model-independent parameterization of possible deviations of this sort.

The SMEFT approach is gauge invariant with respect to the SM gauge group and allows NLO, NNLO, etc. QCD corrections and the NLO or higher electroweak corrections to be calculated self-consistently in each order in the inverse square of the characteristic new-physics scale Λ^{-2}. The examples of calculations and analysis of the obtained constraints given in this review, with the higher-order perturbative contributions taken into account, show the significant role of corrections in reducing uncertainties when imposing bounds on the Wilson coefficients for the SMEFT operators. But there are certain problems in implementing the SMEFT operator constraint program in practice. Even the minimal set of operators (basis) in the SMEFT formalism contains a large number of independent operators and hence a large number of Wilson coefficients that are subject to constraints. With the higher-order perturbative corrections taken into account, there is an additional mixing of operator contributions, which further complicates the analysis. When using SMEFT, it is necessary to exercise certain care in order to not go beyond the applicability limits of the approach, in particular, beyond the boundaries of the unitarity region and the region of applicability of the perturbation theory for effective theories. In the space of parameters (the Wilson coefficients in operators), so-called flat directions can arise, which are linear combinations of coefficients to which experiments either are not sensitive at all or have too low a sensitivity.

But we emphasize that the SMEFT operators given in a unified way allow imposing and comparing constraints on the Wilson coefficients obtained in different analyses of various experimental data. As we have discussed, several groups of theorists have presented the first results of the so-called global fitting of the data of many experiments by theoretical predictions, including the contributions of the maximum possible set of SMEFT operators. In accordance with the general global agreement, the so-called Warsaw basis is most often used in the analysis as a complete set of operators. The SMEFT formalism allows relating data from precision electroweak measurements to data from studies of the Higgs boson, the t quark, and the B, D, and K mesons.

Various extensions of the SM lead to well-defined, extension-specific subsets of operators that can be generated by massive particles, either at the tree level or through their loop contributions. Appropriate studies of the subsets of operators that occur in specific SM extensions are important to better understand which variant of the extensions might be responsible for deviations from the SM predictions if they are found. Such studies, aimed at clarifying the differences among models or, as is common to say, the UV theories, from fitting data with subsets of the corresponding SMEFT operators are at a very early stage of development; the first examples of studies of a number of models are discussed in this review.

The absence of deviations from the SM demonstrates its robustness. At the same time, the SMEFT formalism makes it

possible to model such deviations in a model-independent and theoretically consistent way and thereby increase the chances of their detection. In the absence of deviations, the SMEFT is used for an educated imposition of bounds on the scale and parameters of various UV theories or scenarios. We emphasize that the examples given in this review show that the accuracy of constraints on a number of specific Wilson coefficients is very low, and hence freedom remains for manifestations of new physics in ongoing and planned experiments.

Acknowledgments. The author is grateful to the Russian Foundation for Basic Research for support via grant 20-12-50104. The author is grateful to his colleagues and coauthors V E Bunichev, L V Dudko, M N Dubinin, I P Volobuev, and M A Perfilov, and also to A V Baskakov, who passed away so early, for numerous discussions of the issues explored in this review.

References

1. Lee B W, Quigg C, Thacker H B *Phys. Rev. Lett.* **38** 883 (1977)
2. Lee B W, Quigg C, Thacker H B *Phys. Rev. D* **16** 1519 (1977)
3. Chanowitz M S "Universal W, Z scattering theorems and no-Lose corollary for the SSC", Preprint LBL-21973 (Berkeley, CA: Lawrence Berkeley Laboratory. Univ. of California, 1986); in *Proc. of the 23rd Intern. Conf. on High-Energy Physics, ICHEP'86, 16–23 July 1986, Berkeley, CA, USA* (Ed. S C Loken) (Singapore: World Scientific, 1987) p. 445
4. Dicus D A, Mathur V S *Phys. Rev. D* **7** 3111 (1973)
5. Aad G et al. (ATLAS Collab.) *Phys. Lett. B* **716** 1 (2012); arXiv:1207.7214
6. Chatrchyan S et al. (CMS Collab.) *Phys. Lett. B* **716** 30 (2012); arXiv:1207.7235
7. Beacham J et al. *J. Phys. G* **47** 010501 (2020); arXiv:1901.09966
8. Additional plots of the ATLAS Exotic physics group, https://atlas.web.cern.ch/Atlas/GROUPS/PHYSICS/CombinedSummaryPlots/EXOTICS
9. CMS Exotica Public Physics Results, https://twiki.cern.ch/twiki/bin/view/CMSPublic/PhysicsResultsEXO
10. Weinberg S *Phys. Rev. Lett.* **43** 1566 (1979)
11. Buchmüller W, Wyler D *Nucl. Phys. B* **268** 621 (1986)
12. Appelquist T, Carazzone J *Phys. Rev. D* **11** 2856 (1975)
13. Bogoliubow N N, Parasiuk O S *Acta Math.* **97** 227 (1957)
14. Grzadkowski B et al. *J. High Energy Phys.* **2010** (10) 85 (2010); arXiv:1008.4884
15. Alonso R et al. *J. High Energy Phys.* **2014** (04) 159 (2014); arXiv:1312.2014
16. Gripaios B, arXiv:1506.05039
17. Aguilar Saavedra J A et al., arXiv:1802.07237
18. Boos E et al. *Int. J. Mod. Phys. A* **32** 1750008 (2017); arXiv:1607.00505
19. Boos E E et al. *Phys. Rev. D* **79** 104013 (2009); arXiv:0710.3100
20. Kazakov D I *Phys. Lett. B* **797** 134801 (2019); arXiv:1904.08690
21. Jenkins E E, Manohar A V, Trott M *J. High Energy Phys.* **2013** (10) 87 (2013); arXiv:1308.2627
22. Jenkins E E, Manohar A V, Trott M *J. High Energy Phys.* **2014** (01) 35 (2014); arXiv:1310.4838
23. Zhang C, Maltoni F *Phys. Rev. D* **88** 054005 (2013); arXiv:1305.7386
24. Mebane H et al. *Phys. Rev. D* **88** 015028 (2013); arXiv:1306.3380
25. Chen C-Y, Dawson S, Zhang C *Phys. Rev. D* **89** 015016 (2014); arXiv:1311.3107
26. Zhang C *Phys. Rev. D* **90** 014008 (2014); arXiv:1404.1264
27. Franzosi D B, Zhang C *Phys. Rev. D* **91** 114010 (2015); arXiv:1503.08841
28. Gröber R et al. *J. High Energy Phys.* **2015** (09) 92 (2015); arXiv:1504.06577
29. Hartmann C, Trott M *Phys. Rev. Lett.* **115** 191801 (2015); arXiv:1507.03568
30. Hartmann C, Trott M *J. High Energy Phys.* **2015** (07) 151 (2015); arXiv:1505.02646
31. Zhang C *Phys. Rev. Lett.* **116** 162002 (2016); arXiv:1601.06163
32. Bessidskaia Bylund O et al. *J. High Energy Phys.* **2016** (05) 52 (2016); arXiv:1601.08193
33. Maltoni F, Vryonidou E, Zhang C *J. High Energy Phys.* **2016** (10) 123 (2016); arXiv:1607.05330
34. Gauld R, Pecjak B D, Scott D J *Phys. Rev. D* **94** 074045 (2016); arXiv:1607.06354
35. Degrande C et al. *Eur. Phys. J. C* **77** 262 (2017); arXiv:1609.04833
36. Hartmann C, Shepherd W, Trott M *J. High Energy Phys.* **2017** (03) 60 (2017); arXiv:1611.09879
37. de Florian D, Fabre I, Mazzitelli J *J. High Energy Phys.* **2017** (10) 215 (2017); arXiv:1704.05700
38. Deutschmann N et al. *J. High Energy Phys.* **2017** (12) 63 (2017); *J. High Energy Phys.* **2018** (02) 159 (2018) Erratum; arXiv:1708.00460
39. Baglio J, Dawson D, Lewis I M *Phys. Rev. D* **96** 073003 (2017); arXiv:1708.03332
40. Dawson D, Giardino P P *Phys. Rev. D* **97** 093003 (2018); arXiv:1801.01136
41. Degrande C et al. *J. High Energy Phys.* **2018** (10) 5 (2018); arXiv:1804.07773
42. Vryonidou E, Zhang C *J. High Energy Phys.* **2018** (08) 36 (2018); arXiv:1804.09766
43. Dedes A et al. *J. High Energy Phys.* **2018** (08) 103 (2018); arXiv:1805.00302
44. Dawson S, Giardino P P *Phys. Rev. D* **98** 095005 (2018); arXiv:1807.11504
45. Dawson S, Ismail A *Phys. Rev. D* **98** 093003 (2018); arXiv:1808.05948
46. Dawson S, Giardino P P, Ismail A *Phys. Rev. D* **99** 035044 (2019); arXiv:1811.12260
47. Baglio J, Dawson D, Lewis I M *Phys. Rev. D* **99** 035029 (2019); arXiv:1812.00214
48. Cullen J M, Pecjak B D, Scott D J *J. High Energy Phys.* **2019** (08) 173 (2019); arXiv:1904.06358
49. Neumann T, Sullivan Z *J. High Energy Phys.* **2019** (06) 22 (2019); arXiv:1903.11023
50. Kinoshita T *J. Math. Phys.* **3** 650 (1962)
51. Lee T D, Nauenberg M *Phys. Rev.* **133** B1549 (1964)
52. Grinstein B, Wise M B *Phys. Lett. B* **265** 326 (1991)
53. Peskin M E, Takeuchi T *Phys. Rev. D* **46** 381 (1992)
54. Ellis J et al. *J. High Energy Phys.* **2018** (06) 146 (2018); arXiv:1803.03252
55. Falkowski A, Riva R *J. High Energy Phys.* **2015** (02) 39 (2015); arXiv:1411.0669
56. Heinemeyer S et al. (LHC Higgs Cross Section Working Group), CERN-2013-004 (Geneva: CERN, 2013) http://dx.doi.org/10.5170/CERN-2013-004; arXiv:1307.1347
57. Cepeda M et al. *CERN Yellow Rep. Monogr.* **7** 221 (2019); arXiv:1902.00134
58. Aad G et al. (ATLAS Collab.) *Phys. Rev. D* **101** 012002 (2020); arXiv:1909.02845
59. Sirunyan A M et al. (CMS Collab.) *Eur. Phys. J. C* **79** 421 (2019); arXiv:1809.10733
60. CMS Collab. "Combined Higgs boson production and decay measurements with up to 137 fb^{-1} of proton-proton collision data at $\sqrt{s} = 13$ TeV", CMS-PAS-HIG-19-005
61. Buckley A et al. (The TopFitter Collab.) *J. High Energy Phys.* **2016** (04) 15 (2016); arXiv:1512.03360
62. Gunion J F et al. *Front. Phys.* **80** 1 (2000)
63. Djouadi A *Phys. Rep.* **457** 1 (2008); hep-ph/0503172
64. Marciano W J, Zhang C, Willenbrock S *Phys. Rev. D* **85** 013002 (2012); arXiv:1109.5304
65. Kane G L, Ladinsky G A, Yuan C-P *Phys. Rev. D* **45** 124 (1992)
66. Whisnant K et al. *Phys. Rev. D* **56** 467 (1997); hep-ph/9702305
67. Boos E et al. *Eur. Phys. J. C* **16** 269 (2000); hep-ph/0001048
68. Aguilar-Saavedra J A *Nucl. Phys. B* **804** 160 (2008); arXiv:0803.3810
69. Birman J L et al. *Phys. Rev. D* **93** 113021 (2016); arXiv:1605.02679
70. Boos E, Bunichev V *Phys. Rev. D* **101** 055012 (2020); arXiv:1910.00710

71. Khachatryan V et al. (CMS Collab.) *J. High Energy Phys.* **2017** (02) 28 (2017); arXiv:1610.03545
72. Czakon M, Fiedler P, Mitov A *Phys. Rev. Lett.* **110** 252004 (2013); arXiv:1303.6254
73. Czakon M et al. *J. High Energy Phys.* **2017** (10) 186 (2017); arXiv:1705.04105
74. Kidonakis N *PoS* **247** 170 (2015) https://doi.org/10.22323/1.247.0170; arXiv:1506.04072
75. Sirunyan A M et al. (CMS Collab.) *Eur. Phys. J. C* **79** 886 (2019); arXiv:1903.11144
76. Sirunyan A M et al. (CMS Collab.) *J. High Energy Phys.* **2020** (03) 56 (2020); arXiv:1907.11270
77. Martin A D et al. *Eur. Phys. J. C* **63** 189 (2009); arXiv:0901.0002
78. Kulesza A et al. *Eur. Phys. J. C* **79** 249 (2019); arXiv:1812.08622
79. Aaboud M et al. (ATLAS Collab.) *Phys. Rev. D* **99** 072009 (2019); arXiv:1901.03584
80. Sirunyan A M et al. (CMS Collab.) *J. High Energy Phys.* **2019** (11) 82 (2019); arXiv:1906.02805
81. Aad G et al. (ATLAS Collab.) *Eur. Phys. J. C* **80** 1085 (2020); arXiv:2007.14858
82. Bevilacqua G, Worek M *J. High Energy Phys.* **2012** (07) 111 (2012); arXiv:1206.3064
83. Alwall J et al. *J. High Energy Phys.* **2014** (07) 79 (2014); arXiv:1405.0301
84. Frederix R, Pagani D, Zaro M *J. High Energy Phys.* **2018** (02) 31 (2018); arXiv:1711.02116
85. Hartland N P et al. *J. High Energy Phys.* **2019** (04) 100 (2019); arXiv:1901.05965
86. Biekoetter A, Corbett T, Plehn T *SciPost Phys.* **6** (6) 064 (2019); arXiv:1812.07587
87. Sirunyan A M et al. (CMS Collab.) *J. High Energy Phys.* **08** 11 (2018); arXiv:1711.02547
88. Zhang C, Greiner N, Willenbrock S *Phys. Rev. D* **86** 014024 (2012); arXiv:1201.6670
89. Brivio I et al. *J. High Energy Phys.* **2020** (02) 131 (2020); arXiv:1910.03606
90. Lafaye R et al. *Eur. Phys. J. C* **54** 617 (2008); arXiv:0709.3985
91. Lafaye R et al. *J. High Energy Phys.* **2009** (08) 009 (2009); arXiv:0904.3866
92. Dawson S, Homiller S, Lane S D *Phys. Rev. D* **102** 055012 (2020); arXiv:2007.01296
93. de Blas J et al. *J. High Energy Phys.* **2015** (04) 78 (2015); arXiv:1412.8480
94. Henning B, Lu X, Murayama H *J. High Energy Phys.* **2016** (01) 23 (2016); arXiv:1412.1837
95. de Blas J et al. *J. High Energy Phys.* **2018** (03) 109 (2018); arXiv:1711.10391
96. Das Bakshi S, Chakrabortty J, Patra S K *Eur. Phys. J. C* **79** 21 (2019); arXiv:1808.04403